A New Look at Snowpack Trends in the Cascade Mountains

Mark T. Stoelinga[1], Mark D. Albright, and Clifford F. Mass

Department of Atmospheric Sciences

University of Washington

Seattle, Washington 98195

[1] Corresponding author: Mark T. Stoelinga
                                 University of Washington
                                 Department of Atmospheric Sciences
                                 Box 351640
                                 Seattle, Washington 98115
                 Email: stoeling@washington.edu

Abstract

This study examines the changes in Cascade Mountain spring snowpack since 1930. Three new time series facilitate this analysis: a water-balance estimate of Cascade snowpack from 1930—2007 that extends the observational record 20 years earlier than standard snowpack measurements; a radiosonde-based time series of lower-tropospheric temperature during onshore flow, to which snowpack is well correlated; and a new index of the north Pacific sea-level pressure pattern that encapsulates modes of variability to which Cascade spring snowpack is particularly sensitive.

Cascade spring snowpack declined 23% during 1930-2007. This loss is nearly statistically significant at the 95% level. The snowpack increased 19% during the recent period of most rapid global warming (1976-2007), though this change is far short of being statistically significant due to large annual variability. From 1950-1997, a large and statistically robust decline of 48% occurred. However, 80% of this decline is connected to circulation patterns over the north Pacific Ocean that vary naturally on annual to interdecadal time scales. The residual time series of snowpack after Pacific variability is removed displays a relatively steady loss rate of 2.0% per decade, yielding a loss of 16% from 1930-2007. This loss is statistically significant, and includes the possible impacts of anthropogenic global warming during that period.

The dates of maximum snowpack and 90% melt-out have shifted 5 days earlier since 1930. Both shifts are statistically insignificant. A new estimate of the sensitivity of Cascade spring snowpack to temperature of -11% per °C, when combined with climate model projections of 850 hPa temperatures offshore of the Pacific Northwest, yields a projection of an 8% loss of Cascade spring snowpack due to global warming between 1985 and 2025.

2

1. Introduction

The multi-decadal variation of snowpack in the Cascade Mountains of the Pacific Northwest is an issue of substantial scientific interest, societal impact, and some controversy. Major scientific issues include the magnitude of recent snowpack changes, the dependence of snowpack trends on the period examined, and the importance of natural climate variability versus anthropogenic global warming on past and future snowpack changes. The societal impacts of changes in Cascade Mountain snowpack are significant, since melting mountain snow provides critically needed water resources during the dry summer and early fall months for agriculture, hydroelectric production, maintenance of fish migration runs, and urban water supplies within the heavily populated Puget Sound and Willamette Valley corridors of Washington and Oregon.

A recent scientific report for the state of Oregon (Dodson et al. 2004) suggested a nearly 50% decline of Cascade snowpack has occurred during recent decades, with dates of annual snowpack maximum, melt-out, and streamflow maximum shifting several weeks earlier. An active debate has developed among the local scientific community on this issue, centered on the magnitude and origins of recent snowpack changes. These discussions have been highlighted in the local media[1], and have led to the initiation of relevant new studies focused on Cascade Mountain snowpack (Mote et al. 2008; Casola et al 2009; this paper).

A growing body of literature has examined the multi-decadal trends and variability of snowpack in the Cascade Mountains during roughly the latter half of the 20th century, some as part of larger studies of snowpack in western North America (Cayan 1996; Mote et al. 2005; Hamlet et al. 2005; Mote 2006; Barnett et al. 2008; Pierce et al. 2008) and others more specifically focused

---

[1] Seattle Times, March 15, 2007; Portland Oregonian, February 24, 2007

on the Pacific Northwest or Cascades (Mote 2003; Mote et al. 2008). These studies have found

that spring snowpack in the Cascades experienced large declines (20%-40%) during roughly the

latter half of the 20th century (Mote 2003; Mote et al. 2005, 2008; Hamlet et al. 2005). It was also

found that this decline was due more to warming temperatures than to decreases in precipitation

(Mote et al. 2005, 2008). This conclusion was supported by the observation that percentage losses

of spring snowpack were greater at low elevations than at high (Mote 2003, 2006). Related

studies of spring streamflow for rivers in western North America have found a trend toward earlier

spring pulses during approximately the same period (Cayan et al. 2001; Stewart et al. 2005;

Regonda et al. 2005). Several of the above studies suggest that the observed large losses of

snowpack and earlier spring streamflow pulses in the latter half of the 20th century are due in large

part to anthropogenic global warming (Mote et al. 2005; Stewart et al. 2005; Hamlet et al. 2005;

Mote et al. 2006; Mote et al. 2008).

However, some findings in these studies make the picture less clear, both in terms of the

magnitude and cause of the Cascade snowpack decline. Two studies that examined Cascade

snowpack trends starting prior to 1945 (Hamlet et al. 2005; Mote et al. 2008) found much smaller

losses than trends beginning around 1950. Hamlet et al. (2005), using hydrological model

simulations, found that spring snowpack in the Pacific Northwest has declined only 5% from

1916-2003. Also, trends in Cascade snowpack since 1976, when global temperature records have

shown the steepest warming, show no loss or even a slight gain (Mote 2003; Mote et al. 2005,

2008).

An important contributor to these varying trends is the influence of natural variability in

the north Pacific ocean/atmosphere system on annual to interdecadal time scales, encapsulated in

various climate patterns or indices such as the El Niño/Sothern Oscillation (ENSO), the Pacific

North America pattern (PNA, Wallace and Gutzler 1981), the North Pacific Index (NPI, Trenberth and Hurrell 1994), and the Pacific Decadal Oscillation (PDO, Mantua et al. 1997). In particular, two major shifts in the long-term phase of the PDO in 1947 and 1977 partly explain the downward trend in snowpack during the second half of the 20th century. Several studies have used regression of spring snowpack with one or more of the climate indices mentioned above to assess the contribution of natural climate variability to Cascade snowpack trends (Mote 2006; Mote et al. 2008). These studies found that the existing climate indices explain no more than about 40% of the observed loss of Cascade spring snowpack since 1950, with the implication that the remainder may be attributable to anthropogenic global warming. However, it is not clear that these indices are the best measure of the particular modes of natural variability of the north Pacific atmospheric circulation to which Cascade snowpack is most sensitive, and thus the influence of natural climate variability on Cascade snowpack remains an open question. A goal of this study is to examine natural variability, emphasizing the multiple modes of north Pacific circulation that most strongly affect Cascade snowpack.

Recently, Casola et al. (2009) focused on the sensitivity of snowpack to winter-mean temperature, rather than on analysis of long-term linear trends. Using geometrical, modeling, and observational approaches, they estimated the sensitivity of the Cascade spring snowpack to be 16% loss per °C warming. Applying observed global temperature trends, this sensitivity suggested an 8-16% decline in Cascade snowpack during the past thirty years, which they argue has been masked by large natural variability on annual to interdecadal time scales. Only one of their methods for estimating the sensitivity was based on the observed relationship between snowpack and temperature, and it produced a highly uncertain result due to small sample size and poor correlation between the two variables.

In this study, we develop an estimate of monthly Cascade snowpack based on a simple water balance and high-quality observations of precipitation and streamflow. This new time series extends back to 1930, allowing the examination of trends starting roughly 20 years earlier than has been reliably estimated from direct snowpack observations, and importantly, spanning both known phase shifts of the PDO rather than just one. Using this monthly time series, this paper:

1) examines trends in spring snowpack amount, maximum snowpack date, and 90% melt-out date over three different time periods, and compares the results to previous studies;

2) estimates the sensitivity of Cascade snowpack to lower-tropopsheric temperature; and

3) re-examines the influence of natural Pacific climate variability on Cascade snowpack by seeking circulation patterns that specifically influence Cascade snowpack.

In addition, this study examines the question of how regional lower-tropospheric temperature has changed in recent decades; how it is projected to change over the next few decades by climate model forecasts; and what the implications are for the future of spring snowpack in the Cascades.

2. Data and Methods

a. Streamflow data

A key component of the snowpack estimate developed in this study is a collection of long-term streamflow measurements from rivers draining undisturbed watersheds of the Cascade Mountains (Fig. 1). Most rivers within the Cascades have multiple gauging stations with records extending over many decades. Only a subset of these stations are contained within the Hydro-

Climate Data Network (HCDN, Slack and Landwehr 1992), a set of U.S. gauging stations whose records have been quality controlled and are generally free of anthropogenic contamination by dams, diversions, major land-use changes within the watershed, or measurement errors. For this study, we used the seven HCDN stations within a polygon defining the Cascades (Fig. 1) that have a complete monthly streamflow record spanning water years[2] 1930—2007. The starting year of 1930 was chosen because most of the HCDN gauging stations in the region began recording between 1928 and1930. The boundaries of the upstream drainage area for each gauging station are shown in Figure 1. These drainage areas, subsequently referred to as the "watershed subset", provide a representative sampling of the Cascades in the north-south direction, and include both the east and west sides of the Cascade crest. To produce a single runoff time series for the watershed subset, the monthly runoffs from the seven gauging stations are simply added together, and the total is converted to percent of the 1961-1990 annual mean.

b. Precipitation data

The second key component of the snowpack estimate is precipitation derived from a subset of U. S. Historical Climate Network (USHCN, Karl et al. 1990) stations in the west side of the Cascade polygon and within 10 km of the Cascade foothills. Only precipitation from the west side of the Cascades is used because we found that annual runoff and spring snowpack on either side of the Cascades correlates much better with west-side precipitation than with east-side. This is because most of the heavy snow at high elevations on either side of the crest occurs during westerly flow, when precipitation at low-elevation stations on the west (windward) side is also

---

[2] The "water year" is defined as 1 October through 30 September.

maximized, but low-elevation stations on the east (lee) side are shadowed. The 8 stations chosen (Fig. 1) have a complete monthly record for 1930—2007, and are well distributed in the north-south direction. Despite the tendency for stations to be at low elevations, it will be shown later that they provide a precipitation record that can be calibrated to produce a total precipitation input for the watershed subset. The station precipitation values are converted to monthly percent of normal (1961-1990) and then averaged among the 8 stations to produce a single precipitation time series.

c. Temperature data

The monthly surface temperature records for the 8 USHCN stations are used to provide a surface temperature time series for the watershed subset used in this study. As with precipitation, only west-side temperature observations are used because snowpack on both sides of the crest correlates more highly with west-side winter temperatures than with east-side. The temperature data are converted to anomalies from the monthly station means (1961-1990), and then averaged among the 8 stations to produce a single temperature time series.

850-hPa temperatures and winds from National Weather Service operational soundings on the Washington coast are used to determine how the snowpack is influenced by lower-tropospheric temperatures during onshore flow. Sounding data at Quillayute, Washington (KUIL, Fig. 1) were extracted from the quality-controlled Integrated Global Rawinsonde Archive (IGRA, Durre et al. 2006) for the period 1967-2007. From 1948—1966, soundings were launched from nearby Tatoosh Island (Fig. 1) instead of KUIL. This data is not in the quality-controlled IGRA archive; however, comparisons between the 850-hPa temperatures at KUIL and Tatoosh with the

nearby USHCN site at Forks, Washington indicate that the Tatoosh and KUIL time series are consistent. Upper-air temperatures during 1930-1947 (prior to the start of upper-air observations on the Washington coast) were estimated using a linear regression to the surface temperatures at Forks, which has a correlation of 0.82 with the 850-hPa temperatures at KUIL/Tatoosh during the overlapping periods of record.

d. The water-balance snowpack estimate

This paper utilizes a monthly time series of Cascade snowpack for water years 1930—2007 that was developed by applying a simple water balance equation to the watershed subset. The water balance equates changes in snowpack to precipitation, river runoff, evapotranspiration (ET), and changes in soil moisture. It relies on good measurements of precipitation and runoff, which are the quantities that dominate the monthly water balance in the Cascades, and makes reasonable assumptions about ET and soil moisture change. The details of the method and the assumptions used are described in the Appendix. The end result is an estimated monthly time series of snow water equivalent (SWE) volume within the watershed subset from 1930 to 2007. This estimate of SWE volume will subsequently be referred to as the *water-balance snowpack*, and will be expressed as a percent of the 1961-1990 mean 1 April value.

e. Directly observed snowpack

For the purpose of verifying the water-balance snowpack, the observed monthly snowpack was also estimated for the watershed subset using manual snow course and automated Snow

Telemetry (or "SNOTEL") sites in the Cascades, similar to what was done for a somewhat different area by Mote et al. (2008). The snow course sites provide in situ measurements of SWE depth consistently near 1 April, and less regularly near the first of other months, with a representative network of stations available from the 1950s onward (Mote 2003; Mote et al. 2008); therefore, we use the snow course observations to verify the 1 April water-balance snowpack for the period 1955-2007. The SNOTEL sites provide continuous automated measurements of SWE depth using snow pillows, and thus provide year-round first-of-the-month SWE depth. Because the SNOTEL network began in the mid-1980s, it is used to verify the monthly time series of water-balance snowpack for the period 1984-2007. The snow course and SNOTEL sites used in this analysis were subjected to selection criteria and procedures for filling in missing data similar to those described by Mote et al. (2008). The 82 snow course sites and 50 SNOTEL locations used here are depicted in Fig. 1.

The best estimate of total SWE volume within a region considers the elevation dependence of both SWE depth and areal coverage, rather than simply averaging available SWE depth observations from a variety of elevations (Mote et al. 2008). To account for the variation of areal coverage with elevation, area versus elevation curves[3] (Fig. 3a) were generated for the watershed subset using a 1-km gridded elevation data set. Separate curves were generated for each side of the Cascade crest because they differ significantly below 1000 m elevation. SWE depth versus elevation profiles were estimated east and west of the Cascade crest (Fig. 1) by fitting two lines to the SWE depth vs. elevation scatter plots for all stations within those two areas. An example is shown in Fig. 3b for 1 April SWE depth at snow courses in 2006. All sites in Fig. 1 were used to

---

[3] These curves give the total horizontal area within an elevation band ($z \pm 5$ m) within the watershed subset, as a function of elevation (z). They are proportional to the vertical derivatives of the "hypsometric curves" (not shown), which represent the empirical cumulative distribution function of area vs. elevation in the watershed subset.

produce the linear fits rather than just those within the watershed subset, because only a small fraction are actually within the watershed subset boundaries. The final steps are multiplication of the curves in Figs. 2a and 2b to produce east and west SWE volume versus elevation profiles for the watershed subset (Fig. 3c); summation with respect to elevation to produce single east and west SWE volumes; and summation of those two values to produce a final, single estimate of the total SWE volume within the watershed subset. This procedure is repeated for each year, and is also applied to the monthly observed SWE at SNOTELs. The SWE volume time series are converted to percent of the 1961-1990 mean of the 1 April value.

f. Other data issues

In several of the time series displayed, a smoothed series is shown, representing longer-term variability. The smoothing is performed using a running mean with a Gaussian-shaped weighting function, 5 years wide at half-maximum and truncated at a width of 12 years.

Trends are calculated by subtracting the difference in endpoint values of the least-squares best-fit line over the period in question.   All trends for precipitation and snowpack are expressed as percentages of the 1961-1990 mean value, rather than of the starting value of the trend line. An important component of trend analysis of hydrologic climate parameters is the assessment of uncertainty in the calculated trends due to variability over a finite sampling time (Lettenmaier 1976; Mote et al. 2008; Casola et al. 2009). This uncertainty indicates whether or not a statistically significant secular trend has been detected in a finite time series. We use the formula derived by Casola et al. (2009) for determining the confidence intervals of the trends, utilizing a 95% confidence level and a two-sided test. This formula is based on the Student's *t* distribution,

9

and assumes that the non-trend variability is primarily Gaussian white noise. We have confirmed that the one-lag autocorrelation is small for the time series in question, justifying the latter assumption.

3. Verification of the water-balance snowpack estimate

As a test of the water-balance snowpack estimate, which covers the period 1930-2007, we compare it to the snow course and SNOTEL-derived snowpack estimates described in section 2b, which cover shorter periods but are based on snowpack measurements. Figure 4 shows a scatter plot of 1 April snowpack derived from the snow course observations during the period 1955—2007 (x-axis) versus the 1 April water-balance snowpack (y-axis). A high correlation of 0.95 is achieved, and the points lie very close to the 1:1 line. This agreement is remarkable considering the two estimates are derived from completely different observations, and somewhat different watersheds. The agreement is a testament to the spatial consistency of the hydrological water balance throughout the region of interest. The 1955—2007 linear trends from the water-balance and snow course-based snowpack (Fig. 4) are within 3% of each other. The correlation with observed snowpack and agreement with observed snowpack trends using the water balance approach are at least as good as those produced by hydrologic model simulations (Mote et al. 2008).

An important consideration is how well the watershed subset used to produce the water-balance snowpack estimate represents the Cascades as a whole. Although regionally averaged precipitation was used in developing the water-balance snowpack time series, the runoff observations are only from the watershed subset, and those watersheds have different

characteristics than the Cascades as a whole. Specifically, the area-versus-elevation profile of the watershed subset (Fig. 2a) is skewed toward higher elevation than the full Cascade profile (not shown, but calculated using elevation data within the full Cascade polygon in Fig. 1). To test the potential sensitivity of the water-balance snowpack to the elevation characteristics of the watershed subset, the snow course-based snowpack time series was regenerated using the area versus elevation function for the entire Cascades. The 1955-2006 trend in 1 April snowpack calculated using the full Cascade profile was -35%, only a slightly larger decline than the -31% decline obtained using the watershed subset profile. These results instill confidence that the water balance method applied to the watershed subset yields a snowpack estimate that is applicable to the Cascades as a whole.

One purpose of the water-balance snowpack is to exploit its monthly time resolution to examine parameters like date of maximum snowpack and melt-out date. To verify the monthly behavior of the water-balance snowpack, we compared it to the SNOTEL-derived snowpack, which also has monthly time resolution, but only for 1984-2007. The two monthly time series during a subset of this period (1992—2007) are shown in Fig. 5. In general, the water-balance snowpack tracks the SNOTEL-estimated snowpack closely in terms of the timing and magnitude of the maxima and the annual melt-out. Occasionally the water-balance snowpack exhibits some erratic small-amplitude perturbations around the time of maximum snowpack (e.g., water years 1993, 1995, and 2005), which can result in unrealistically early dates of maximum snowpack, but these years are uncommon.

Overall, these verification results provide confidence that the water-balance snowpack can be used to assess the long-term behavior of 1 April Cascade snowpack and the timing of maximum snowpack and melt-out. These assessments are the subject of the next section.

4. Results

a. Snowpack trends

The full record of the water-balance snowpack on 1 April for the Cascades is shown in Fig. 6a. The unsmoothed time series shows considerable annual variability, ranging from a maximum of 191% of normal in 1956 to a minimum of 18% of normal in 2005. Trends were calculated over three periods. Over the full period of record (1930-2007), the trend is -23%, although this trend is not quite statistically significant (as indicated by the 95%-confidence interval of ±28%), due to the large variability of the snowpack. The second period is 1950-1997, which was used by Mote et al. (2005) to demonstrate large declines in snowpack in western North America, but is also a period that spans a known shift in the PDO from its "cool" to "warm" phase in 1977. In that year there was a large shift from a high to a low snowpack regime over the Pacific Northwest (Cayan 1996; Mantua et al. 1997). The water-balance snowpack trend reflects this PDO modulation during the 1950-1997 period, showing a large, statistically significant decline of 48%, much of it associated with the cool-to-warm PDO shift in 1977. Further analysis of the connection of the snowpack to natural Pacific climate variability will be presented later. The third time period is 1976-2007, which is of unique interest because it is entirely after the cool-to-warm PDO shift of 1977, and coincides with a period of particularly rapid increase in global mean surface temperatures, as indicated by analyses such as that of the Hadley Centre/Climatic Research Unit (Brohan et al. 2006). The most recent IPCC report (IPCC 2007) ascribed much of this recent global warming to anthropogenic increases in greenhouse gases. In spite of the rapid global warming, this period

saw a 19% *increase* in snowpack in the Cascades, although this trend falls far short of the large

(43%) threshold required for statistical significance, due to the short period considered and large

annual variability of the snowpack.

b. Relationship between snowpack, precipitation, and temperature in the Cascades

Before examining the relationship of snowpack to precipitation and temperature, it is

instructive to examine the relevant precipitation and temperature records. The precipitation

averaged over the west side of the Cascades, accumulated from October through March (hereafter

referred to as P, and shown in Fig. 6b) exhibits considerable interannual variability, though

somewhat less than snowpack (Fig. 6a). The extremes are 50% of normal (1977) and 145% of

normal (1997). Precipitation trends over all three time periods discussed above are small and not

statistically significant. Figure 6c shows the Cascade west-side winter-averaged (November-

March) surface temperature record, T_s. All three periods show positive slopes, and the upward

trends are similar to those of the winter (November-March) global-mean surface temperature[4] over

the same period, which were +0.08 °C per decade during 1930-2007, +0.09 °C per decade during

1950-1997, and +0.19 °C per decade during 1976-2007 (not shown).

In their analysis of the sensitivity of Cascade snowpack to winter temperature, Casola et al.

(2009) discuss the distinction between a simple winter-average of the local temperature (such as T_s

described above), and a temperature that is weighted according to when precipitation is falling,

with the latter being more relevant to determining the phase (snow or rain) of the accumulated

precipitation. We hypothesize, based on extensive personal experience, that since much of the

---

[4] These trends are from the monthly global-mean surface temperature time series provided by the
Hadley Centre/Climatic Research Unit, described in Brohan et al. (2006).

winter precipitation in the Cascades falls when cold, moist westerly to northwesterly flow in the lower troposphere impinges directly on the Cascade barrier. Therefore, a better discriminant of precipitation phase than surface temperature might be the winter mean temperature at 850 hPa (roughly 1500 m above sea level) for periods when the 850-hPa flow has an onshore component (T_{850ons}). A potential added benefit of using the upper-air temperature is the reduction of contamination due to changing site characteristics and urbanization that can affect surface stations. A time series of 850 hPa temperature (Fig. 6d) shows many of the variations seen in the T_s record, but with several important differences, including more pronounced interdecadal features, like the steep increase for 1950-1997, and little trend during the recent period of rapid global warming (1976-2007). It will be shown later that these temporal characteristics reflect the interdecadal-scale climate variability of the northern Pacific Ocean.

Scatter plots of 1 April snowpack with winter precipitation, surface temperature, and 850-hPa temperature during onshore flow, along with correlations, are shown in Fig. 7. The higher correlation with precipitation (0.80) than with surface temperature (-0.44) is consistent with results of Mote (2006) and Mote et al. (2008). A substantially larger correlation is obtained with T_{850ons} (r = -0.67) than with T_s (r = -0.44), suggesting that T_{850ons} provides a better estimate of the winter temperature relevant to Cascade snowpack than does T_s.

Mote (2006) and Mote et al. (2008) have used multiple linear regression to analyze the separate contributions of winter temperature and precipitation to changes in 1 April SWE depth observed at snow courses in western North America. A similar analysis is performed here, using the water-balance snowpack estimate for the Cascades. Specifically, multiple linear regression is used to find the best fit of the following linear relationship between the snowpack, precipitation, and temperature data:

$$S = (a_1 P + a_2 T + a_3) + S_{\text{res}} = S_{\text{fit}} + S_{\text{res}}. \qquad (1)$$

The a terms are the regression coefficients, including the intercept a_3. The goodness of fit is measured by the correlation of the fitted snowpack value, S_{fit}, with the total snowpack, S. The part of the total snowpack that is uncorrelated with the predictor variables, or the "residual", is designated S_{res}.

Application of multiple linear regression using P and T_s in (1) yielded a correlation of 0.87, whereas using P and $T_{850\text{ons}}$ yielded a higher correlation of 0.90. One might have expected an even larger improvement with $T_{850\text{ons}}$, considering the substantially larger correlation of snowpack (in single regression) with $T_{850\text{ons}}$ (Fig. 7c) than with T_s (Fig. 7b). The reason for the modest additional correlation is because the cross-correlation between temperature and precipitation is higher using $T_{850\text{ons}}$ ($r = -0.37$) than using T_s ($r = -0.13$), i.e., $T_{850\text{ons}}$ takes advantage of some additional correlation between $T_{850\text{ons}}$ and P. A more rigorous way to compare $T_{850\text{ons}}$ with T_s is by examining their partial correlations with snowpack. Partial correlation [see Panofsky and Brier (1963), pp. 114-116] is the correlation of one variable (for example, T_s) with another variable (in this case, snowpack) when the influence of a third variable (in this case, P) has been removed from the other two. The partial correlations of T_s and $T_{850\text{ons}}$ with snowpack are, respectively, -0.57 and -0.68, indicating that $T_{850\text{ons}}$ does provide additional information over T_s, independent of P.

The multiple linear regression results are shown in Table 1. Over the full period of record (1930-2007), most of the 23% decrease in snowpack is associated with warming temperature. Warming plays an even larger role in the large decline in snowpack during 1950-1997, and the decline is enhanced by a decrease in precipitation during this period. However, during the period of recent rapid global warming (1976-2007), the slight decline in $T_{850\text{ons}}$ (Fig. 6d) results in little

temperature contribution to snowpack changes, leaving the increasing precipitation to dominate and produce an increase in snowpack. Examination of the residual for all three periods indicates a nontrivial contribution to the trend in 1 April snowpack (ranging from -11 to +5%) due to random errors in all three measurements and the exclusion of other factors (Mote et al. 2008)[5].

As mentioned previously, Casola et al. (2009) examined the sensitivity of the Cascade snowpack (S) to a unit change in mean winter temperature (T), expressed as percent change in S per unit change in T. They defined this sensitivity as:

$$\lambda = \frac{dS}{dT} = \frac{\partial S}{\partial T} + \frac{\partial S}{\partial P}\frac{dP}{dT} = \lambda_{\text{direct}} + \lambda_{\text{feedback}}. \tag{2}$$

In other words, the total sensitivity is the sum of the direct sensitivity to temperature (T) holding precipitation (P) constant, and any feedback due to a relationship between T and P. They estimated λ_{direct} by four different methods, finding an average value of 20% $^\circ\text{C}^{-1}$. The only method that involved measurements of snowpack and temperature was the one based on single linear regression of observed snowpack and temperature, which yielded a value of 27 ± 15 % $^\circ\text{C}^{-1}$. The large uncertainty in this estimate was due to a short period of record (1970-2006) and a low correlation between temperature and snowpack ($r = -0.52$). Here we repeat this approach using $T_{850\text{ons}}$ and the longer time period of the water-balance snowpack time series. λ_{direct} is, by definition, the regression coefficient for $T_{850\text{ons}}$ produced by multiple linear regression of S with $T_{850\text{ons}}$ and P, since that regression coefficient is the slope of S with respect to $T_{850\text{ons}}$ holding P constant. By this definition, $\lambda_{\text{direct}} = -15$ % $^\circ\text{C}^{-1}$. To calculate the 95% confidence interval on the

---

[5] The residual produced during the full period of record (1930-2007) when using $T_{850\text{ons}}$ in the multiple linear regression (-11% of normal snowpack, Table 1) was less than that produced when using T_s (-16% of 1961-1990 mean snowpack, not shown), further supporting the choice of $T_{850\text{ons}}$ as a more relevant temperature parameter for spring snowpack in the Cascade Mountains.

sensitivity, we use the partial correlation of $T_{850\text{ons}}$ and S holding P constant, previously given as

-0.68, and the same Casola et al. (2008) formula for confidence intervals discussed previously.

This yields a 95% confidence interval of ± 4%, considerably smaller than that obtained by Casola

et al. Our smaller uncertainty is due to a longer period of record, better partial correlation of S

with $T_{850\text{ons}}$ than with T_s, and elimination of precipitation-induced variability using multiple linear

regression. Adding in the Casola et al. estimate that $\lambda_{\text{feedback}}$ may be as high as +4 % °C^{-1} yields λ

= -11 ± 4% °C^{-1}, a somewhat lower estimate of the sensitivity than that given in Casola et al. (-16

% °C^{-1}). One caveat is that there is little understanding of how global warming has produced, or

will continue to produce, more complicated climatic responses such as changes in storm

intensities, storm tracks, natural modes of variability such as ENSO and PDO, etc. All of these

unknowns add to the uncertainties in the magnitude, and perhaps even the sign, of $\lambda_{\text{feedback}}$.

c. Relationship between Cascade snowpack and natural interdecadal-scale variability

The North Pacific Index, or NPI (Trenberth and Hurrell 1994), is an atmospheric index that

is thought to encapsulate much of the atmospheric variability associated with the PDO, as well as

ENSO. It is defined as the mean sea-level pressure (SLP) (minus 1000 hPa) in the north-central

Pacific Ocean (see box in Fig. 8a), and can be thought of as a measure of the strength of the

Aleutian Low. It can be argued that the PDO reflects primarily natural climate variability,

supported by the fact that the linear trend of the NPI explains less than 3% of its variance during

1930-2007, compared to, for example, the global surface temperature, whose linear warming trend

explains over 50% of its variance during the same period. Some studies have suggested that the

amplitude and frequency of ENSO, to which the PDO is closely related, are influenced by anthropogenic global warming, but this question is a matter of ongoing debate (Guilyardi 2006).

Mote (2006) and Mote et al. (2008) have concluded that natural climate variability explains only about 40% of the losses in Pacific Northwest spring snowpack during the latter half of the 20th century, based on linear regression of snowpack with the NPI and removal of its influence from the snowpack time series. We performed a similar analysis with the water-balance snowpack, and obtain a similar result: the loss during 1950-1997 is reduced from 48% to 29% (a relative reduction of 39.6%). However, significant annual to interdecadal variability remains in the residual snowpack time series (not shown), suggesting that the NPI is an imperfect index of the natural Pacific climate variability that is relevant specifically to Cascade snowpack. It is entirely reasonable to suspect that there are multiple modes of natural climate variability in the north Pacific that affect Cascade snowpack that cannot be represented by a simple box-average of SLP over the north-central Pacific Ocean.

To investigate this hypothesis, we sought an alternate SLP-based north Pacific atmospheric circulation index that includes multiple modes of Pacific climate variability to which Cascade snowpack is particularly sensitive. Using the gridded historical monthly mean SLP data set (5°x5° resolution) produced by the Hadley Centre (Allan and Ansell 2006), we constructed a map over the north Pacific Ocean of the regression coefficient between November-March mean SLP and 1 April Cascade snowpack during the period 1930-2007 (Fig. 8a). The most prominent "center of action" in this map is a high positive correlation with SLP within the Aleutian Low (high SLP = weak Aleutian Low = high Cascade snowpack), centered near 50°N, 175°W. This is the same connection between Cascade snowpack and north Pacific circulation that is captured by the winter-mean NPI (defined as the average SLP within the box in Fig. 8a). However, there are

clearly two other centers of action closer to the West Coast: a region of negative correlation (low pressure = high Cascade snowpack) extending from the Alaska Panhandle southeastward into the northwestern U.S., and a region of positive correlation (high pressure = high Cascade snowpack) off the coast of southern California. The two west-coast centers of action make sense in that they both contribute to a stronger cross-barrier geostrophic flow in the Cascades.

To what degree do these three centers of action represent independent modes of variability? To investigate this question, a method was devised to identify the three points within the domain of Fig. 8a that are maximally independent from each other but also maximally correlated with Cascade snowpack (via multiple linear regression). The method is similar to the technique described by Van Den Dool et al. (2000) for identifying "empirical orthogonal teleconnections." First, the grid point with the highest correlation of SLP to Cascade snowpack was identified as "point 1", representing the first center of action. Using linear regression, the influence of SLP at point 1 was then removed both from the snowpack time series and from the SLP time series at all other grid points, and a new correlation map between the residual snowpack time series and the remaining SLP field was produced. The new point of highest correlation was identified as "point 2", which was near the second center of action. The procedure was repeated again to find "point 3", roughly near the third center of action as expected. The procedure could have been repeated to find points 4, 5, etc., but it was found that little additional variance in snowpack was explained beyond the third point. The final three points obtained[6] are those shown in Fig. 8, located at 50°N/170°W, 50°N/135°W, and 20°N/125°W.

---

[6] It is possible that point 1 could change if it is re-identified after points 2 and 3 are known and accounted for, so a refinement procedure was applied to each of the three points in sequence to insure that they were each at the point of maximum correlation between SLP and snowpack when the influence of SLP at the other two points was removed from the snowpack and SLP time series. Additionally, a more laborious experiment was conducted in which every possible set of three

19

The total correlation of snowpack with SLP using the three points (via multiple linear regression) is $r = 0.84$ ($r^2 = 0.71$), and the additional fractional variance explained by incrementally adding each point to the multiple regression is 0.35, 0.24, and 0.12, respectively. In other words, the second (Alaska Panhandle) and third (California) points together explain about the same amount of variance as the first point (Aleutian Low, similar to NPI). SLP time series at the three points are not highly correlated with each other ($r_{12} = 0.36$, $r_{23} = 0.04$, and $r_{31} = 0.11$), confirming that they describe largely independent modes of variability.

The result of the multiple linear regression applied to the winter-mean SLP time series at the three "best" points identified above can be used to construct a "Cascade Snowpack Circulation" index, referred to hereafter as the CSC index, to distinguish it from the NPI:

$$\text{CSC index} = 0.5985 \times SLP_1 - 0.7349 \times SLP_2 + 1.8382 \times SLP_3 - 1724.8 \text{ hPa}, \quad (3)$$

where the SLP values are in hPa.

To help understand how the CSC index, as defined in (3), relates to snowpack in the Cascades, Fig. 8b shows a composite of the anomaly of the winter-mean SLP field in the 5 years with the highest CSC index during 1930-2007. The composite SLP anomaly field roughly mirrors the correlation map (Fig. 8a), and resembles the negative of a composite winter 700-hPa anomaly pattern for low 1 April snowpack years in Oregon found by Cayan (1996). A weak Aleutian Low (high SLP anomaly) is coupled with low pressure along the west coast of Canada and higher pressure off of southern California. The composite SLP anomaly for the 5 years of lowest CSC index (not shown) is essentially equal and opposite of Fig. 8b. Also shown are the full winter-

---

points in the domain was examined to see which set's SLP times series described the largest fraction of SWE variance (via multiple linear regression), and that experiment produced the same result as the iterative procedure described herein, although the iterative procedure found the three points in a fraction of the processor time. It is likely, though not certain, that the two procedures would always identify the same set of points in general.

mean SLP field during the five highest (Fig. 8c) and lowest (Fig. 8d) CSC index years. In high index/snowpack years, the SLP field offshore of the Pacific Northwest is characterized by nearly zonal geostrophic flow that impinges directly onto the Pacific Northwest coast. In low index/snowpack years, the geostrophic flow is stronger offshore, but the flow follows a southwest to northeast course toward the Alaska Panhandle, bypassing the Washington/Oregon Cascades and leaving them in a more quiescent and warmer regime.

An annual time series of the winter-mean CSC index is shown in Fig. 9a, with mean values during the PDO epochs shown by horizontal bars. The CSC index shows pronounced PDO epoch transitions at 1947 and 1977, more so than the NPI (not shown), whose PDO epoch transitions are more subtle. A scatter plot of 1 April Cascade snowpack versus CSC index (Fig. 9b) illustrates the close correspondence between the two variables, and a time series of 1 April Cascade snowpack after the influence of the CSC index is removed (Fig. 9c) shows a highly reduced variability compared to the full snowpack time series (Fig. 6a). Furthermore, the residual trends in 1 April snowpack over the shorter 1950-1997 and 1976-2007 periods (listed in Fig. 9c) become very consistent with the trend during the full period, unlike the full snowpack times series. The residual trend shows a remarkably steady loss of snowpack at a rate of ~2.0% per decade. We postulate that it is this residual trend in Cascade 1 April snowpack that may be due in part to the effects of anthropogenic global warming.

The residual snowpack loss of -16% from 1930-2007 is statistically significant (Fig. 9c), indicating that a downward trend not attributable to natural interdecadal variability of the Pacific climate system has been detected. A recent study by Pierce et al. (2008) using long-term climate simulations and a formal detection and attribution approach suggested that snowpack loss in the western U. S. since 1950 already exceeded that explainable by natural variability in the early

1990s. There are a few possible explanations for the much shorter time period of detection found in their study. First, although the spatial patterns and magnitude of variability in Pacific SST and western snowpack in Pierce et al.'s control climate simulations compared favorably with observations, what was not demonstrated was the ability to produce the robust "polarity reversal" behavior associated with the PDO on interdecadal time scales, like those that were observed in 1925, 1947 and 1977 (Mantua et al. 1997). Therefore, their control climate simulations may not have adequately represented the potentially large natural trends in snowpack that can occur over a time period that straddles one of these polarity shifts, such as the 1950-1999 time period used by Pierce et al. Additionally, they examined the snowpack behavior in the entire western United States, whereas we focused on the Cascade Mountains, which are known to be more strongly influenced by natural Pacific climate variations than other regions of the west (Stewart et al. 2005).

d. Trends in maximum snowpack date and melt-out date

Recently Hamlet et al. (2005) carried out simulations with the Variable Infiltration Capacity (VIC) hydrology model (Liang et al. 1994) over western North America for the 20th century, and found that in some locations, including several in the Cascades, the date of maximum snowpack has moved 15-45 days earlier in the year, and that the date of 90% melt-out has moved 15-40 days earlier. However, these results were for the small subset of points that showed the largest shifts to earlier dates. Here we examine whether such large shifts toward earlier maximum snowpack and melt-out are evident in our water-balance snowpack record for several watersheds in the Cascade Mountains from 1930 to 2007.

The estimation of daily maximum snowpack and melt-out dates from the monthly snowpack time series requires an interpolation from first-of-month data to a daily time series, which is accomplished with a cubic-spline interpolation[7]. Melt-out is defined here as in Hamlet et al. (2005), i.e., the Julian date at which each year's snowpack is reduced by 90% of that year's peak value. The maximum and melt-out date time series, based on the water-balance snowpack, are shown on the same graph with Julian date on the *y*-axis (Fig. 10), with the trends and uncertainties given for the three time periods. Both dates exhibit considerable annual variability, especially the melt out date. The trends are qualitatively similar to those found for 1 April snowpack (Fig. 6a), although the full-record (1930-2007) trends are less remarkable. Specifically, the dates of both maximum snowpack and 90% melt-out occur just 5 days earlier in 2007 than they did in 1930, with the threshold for a statistically significant change being two weeks. Shifts of these dates during 1950-1997 are larger (tending toward earlier maximum and melt out). These results are consistent with findings of earlier spring streamflow pulse during approximately the same 1950-1997 period (Cayan et al. 2001; Stewart et al. 2005; Regonda et al. 2005), but are strongly influenced by Pacific variability, as was the case for the snowpack decline during this period (see previous section), Trends during the recent period of accelerated global warming (1976-2007) are for *later* maximum snowpack and melt out dates, though uncertainty in the linear

---

[7] The use of a cubic spline interpolation to convert a monthly to a daily time series of snowpack potentially can introduce error into the time series and additional uncertainty into the trends for dates of maximum snowpack and melt out. We tested this error using a SNOTEL time series with daily resolution, comparing it to time series interpolated from a monthly sampling and found that the error in melt-out date is random with a standard deviation of 5.5 days. This translates to an additional uncertainty (at the 95% confidence level) of ±4 days in the trend of melt-out date from 1930-2007, which is considerably smaller than the variability-induced uncertainty listed in the upper left part of Fig. 10 (±20 days).

trend during this period is much larger than the trend itself, as was true for 1 April snowpack. The magnitudes of all the trends are reduced when the influence of the CSC Index is removed from the time series (not shown).

5. Relationship of Cascade snowpack to past and future regional temperature changes

Section 4 showed that the temperature of lower-tropospheric onshore flow is highly correlated with the build-up of the Cascade snowpack during winter storms. This is consistent with conventional knowledge that much of the snowfall in the Cascades occurs during a synoptic-scale regime of strong westerly (cross-barrier) flow in the lower troposphere, which is usually accompanied by an ideal combination of cold temperatures, plentiful moisture, and weakly stable lapse rates. The 850-hPa winter temperature during onshore flow exhibited little trend during the recent period of rapid global warming (Fig. 6d). This flat trend, although rendered uncertain by large annual variability in the timer series, is nonetheless consistent with weak surface air temperature trends over a broad region of the northeastern Pacific offshore of the Pacific Northwest, as seen in a map of the 1976-2007 trends in December-February mean surface air temperature (Fig. 11) produced using the global surface temperature data set of Hansen et al. (2001). This broad region of relatively small temperature trend offshore of the Pacific Northwest, compared to larger increases elsewhere in the Northern Hemisphere, has likely contributed to a lack of decline in Cascade snowpack since 1976.

As was done in Casola et al. (2009), one can attempt to project future changes in Cascade spring snowpack by multiplying the estimated sensitivity with a projection of temperature change based on climate model simulations. Recently, Overland and Wang (2007) examined the coupled

ocean-atmosphere climate model forecasts used in the *IPCC AR4* report (using the A1B emission scenario), and identified a group of model forecasts that best captured the observed decadal-scale variability over the northeastern Pacific Ocean during the 20th century. Figure 12 shows the pattern of the projected change in mean November-March temperatures over the northern Pacific Ocean during 1990-2025 in Overland and Wang's ensemble, for the sea surface, surface air, and air aloft (850 hPa). All three of these temperature trend patterns suggest that the region offshore of the Pacific Northwest will continue to warm at a slower pace than most other areas around the Pacific Basin. However, it can also be seen that projected warming at 850 hPa is generally larger than at the surface. The projected 850 hPa temperature change at the Washington coast from 1990 to 2025 (+0.75 °C , or 0.21 °C per decade) is close to the global-mean surface temperature change projected over the same period by the IPCC (+0.80 °C , or 0.23 °C per decade). It is also about twice the rate of warming of T_{850ons} observed from 1930 to the present (+0.12 °C per decade, Fig. 6d). Applying the 850 hPa warming rate of 0.21 °C per decade projected by Overland and Wang's ensemble, and the snowpack sensitivity derived in section 4b of -11 % °C^{-1}, yields a loss for the next few decades of around -2.3% per decade. An estimate of cumulative loss of Cascade snowpack from 1985—2025 that is potentially due to global warming can be projected by starting with the loss not attributable to circulation changes that has already occurred through 2007 (-2.0% per decade, section 4c) x 2.2 decades = -4.4%. To this is added the projected additional loss of 2.3% per decade x 1.8 decades (2007-2025) = 4.1%, for a total of 9%. This is considerably smaller than the 29% loss from 1985-2025 recently projected for the Washington Cascades and Olympics in the *Washington Climate Change Impacts Assessment* (Chapter 3, Elsner et al. 2009), based on hydrologic model simulations driven by a downscaled climate model ensemble.

6. Conclusions

In this study, we have considered the trends in snowpack and related parameters in the Cascade Mountains from 1930-2007. A major tool has been a simple water-balance method for estimating monthly Cascade Mountain snowpack from high-quality streamflow and precipitation measurements. This snowpack estimate extends back to 1930, well before the start of reliable direct snowpack observations, and also well before the large 1947 shift in the Pacific Decadal Oscillation (PDO). The water-balance snowpack record was analyzed in terms of its trend over various time periods, its relationship to temperature, precipitation, Pacific interdecadal climate variability, and its implications for projected climate change in the northeast Pacific Ocean region. The analysis yielded the following conclusions:

1) The water-balance snowpack estimate verified well against observations, and represents an alternative to hydrological modeling for producing a historical monthly record of snowpack when high-quality, long-term climate observations of precipitation and streamflow are available.

2) Using the water-balance Cascade snowpack, the overall trend in Cascade spring snowpack over the entire period of record (1930-2007) is -23% of the 1961-1990 normal, although this trend does not quite meet the 95% confidence level for a non-zero trend. The trend is primarily a result of warming, as precipitation showed little trend during this period.

3) The loss in snowpack during the period 1950-1997, when the PDO shifted from a cool to a warm phase, was a statistically significant 48%, attributable to warming and, to a lesser extent, a decline in precipitation.

4) The spring snowpack trend during the recent period of relatively rapid global temperature increase (1976-2007) was marked by *increasing* Cascade spring snowpack, although the trend is well short of the threshold for statistical significance at the 95% level, due to the short time period considered and large annual variability in snowpack.

5) Better correlations of snowpack with temperature and precipitation were obtained, and smaller residual trends remain, when multiple linear regression of snowpack is performed using the winter-mean 850-hPa temperature upwind of the Cascades during onshore flow at that height, rather than the winter-mean surface temperature in the Cascade Mountains. This suggests that the 850-hPa temperature during onshore flow is a key controlling temperature for the phase of Cascade precipitation and the buildup of snowpack. The recent three decades have seen little increase in this temperature parameter, consistent with little change in Cascade snowpack during that period, and the lack of warming of the eastern Pacific.

6) Using the winter-mean temperature at 850 hPa during onshore flow, we estimate the sensitivity of Cascade snowpack to temperature to be approximately -11 ± 4 % $°C^{-1}$, somewhat less than the recent estimate by Casola et al. (2009) of -16 % $°C^{-1}$.

7) The large 48% decline in Cascade snowpack between 1950 and 1997 is mostly attributable to natural variability of the north Pacific region. The North Pacific Index (NPI), which is one measure of Pacific atmospheric climate variability, explains less than 50% of this downward trend. However, a new "Cascade Snowpack Circulation" index, that accounts for multiple modes of variability in the winter-mean north Pacific sea-level pressure field that most strongly affect Cascade snowpack, explains about 80% of the downward trend in spring snowpack during this period. The residual snowpack time series displays a modest

steady loss rate of 2% per decade. The total residual loss from 1930-2007 is 16%, and is statistically significant. Some portion of this residual loss may be due to anthropogenic global warming.

8) During the 78-year record of the water-balance snowpack time series (1930-2007), the dates of maximum snowpack and 90% melt-out both shifted earlier in the year by 5 days. Neither of these shifts is statistically significant.

9) An ensemble of coupled climate model simulations for the next several decades projects that the temperatures at 850 hPa over the northeastern Pacific Ocean will warm at a rate of roughly 0.21 °C per decade. Combining this warming rate with our observationally based sensitivity calculation yields a projection that from 1985-2025, cumulative loss of Cascade spring snowpack will be 9%, which is considerably less than the 29% loss projected for the same period by a recent climate impacts report for Washington state.

Appendix: The water-balance snowpack estimate

The snowpack estimate is based on a simple water balance equation for a watershed (or group of watersheds) over some specified time period:

$$\Delta S = P - E - R - \Delta M , \qquad (4)$$

where ΔS is the change in snow water equivalent volume, P is precipitation, E is evapotranspiration (or ET), R is runoff (assumed to be equal to gauge-measured streamflow), and ΔM is the change in soil moisture (including ground water) over the period in question. The goal is to apply this equation on a monthly basis to the watershed subset to obtain monthly ΔS. In terms of direct volume measurements for the watershed subset, only R is available. The west Cascade USHCN stations (Figure 1) provide an uncalibrated value of total precipitation volume in the watersheds, P_u, which is not the same as the true precipitation volume in the watersheds, P, but is assumed to be proportional to it. Calibration of the precipitation is necessary to account for effects such as the elevation dependence of precipitation, watershed area, and gauge undercatchment, To calibrate P_u, we first consider the application of (4) to the watershed subset for a full water year (rather than on a monthly time scale). To a good approximation, the annual changes of snowpack and soil moisture are essentially zero, since there is typically little of either remaining at the end of the water year (compared to the maximum amount). Therefore, the annual water balance can be approximated by

$$R = P - E = bP_u - E , \qquad (5)$$

where b is the calibration constant that allows the use of the measured Cascade-mean precipitation over the watershed subset. A scatter plot of R (the annual water-year runoff in the watershed subset) versus P_u (Fig. 2) produces a high correlation, 0.94, motivating the use of the linear relationship to calibrate the precipitation. Note that the line does not intersect the origin, and the negative intercept, E_0, represents water that does not go into runoff. It would be tempting to simply assume that this constant amount represents the total annual ET. This implies that annual ET is 30% of mean annual runoff. However, long-term hydrological model simulations applied to Cascade watersheds[8] indicate that mean annual ET in the Cascades is larger, around 49% of mean annual runoff. To account for this discrepancy within the context of the nearly linear relationship between R and P_u, we define an estimate of ET that includes both E_0 and an additional part that is proportional to annual precipitation:

$$E_{\text{est}} = aP + E_0 = abP_u + E_0. \qquad (6)$$

Substituting this into (5), applying the result to the 1930-2007 means (overbars) for R and P_u, (i.e., the means of the y and x data points, respectively, in Fig. 2) and assuming the ratio $\eta \equiv \overline{E} / \overline{R} = 0.49$ as suggested above, we obtain:

$$b = (1+\eta)\overline{R} / \overline{P_u} = 1.51 \quad \text{and} \quad a = 1 - (\overline{R} + E_0) / (b\overline{P_u}) = 0.131. \qquad (7)$$

These values can then be used to calibrate the annual precipitation ($P = bP_u$). Once the calibrated precipitation volume into the watershed subset is known, a better estimate of annual ET can be obtained by solving (5) for E. This estimate of ET is equal to the linear fit-based estimate from

---

[8] A. Wood (University of Washington) has provided climatological water balance data from simulations using the VIC hydrologic model within several Cascade Mountain watersheds during the period 1971—2000, described in Wood and Lettenmaier (2006). Those watersheds were similar in location to, but not the same as, the "watershed subset" used in the present study.

(6), minus the annual residual in streamflow (the vertical excursion of each data point from the line in Fig. 2), which importantly includes any long-term trend in annual ET related to warming. In fact, the method yields a small positive trend in ET from 1930-2007, which is balanced by a small downward trend in snowpack that is included in the snowpack time series shown in this paper.

To produce the monthly time series, all terms in (4) must be accounted for. The monthly runoff is known, and the monthly precipitation is assumed to calibrate with the same constant as the annual precipitation [i.e., the b constant, as calculated in (7)]. Although the annual ET can be estimated with (6) and (7), this amount must be distributed among the months of the water year, and an additional assumption must be made about the monthly change in soil moisture. A reasonable approach is to assume that the monthly sum of E and ΔM follows the monthly climatologies of these quantities, multiplied by a constant of proportionality so that the annual total equals the annual total E already calculated (with the annual total of ΔM assumed to be zero, as mentioned previously). We utilize a climatology of these terms (Fig. 13) that was derived from the previously mentioned long-term hydrological model simulations for the Cascades. We tested the sensitivity of the snowpack estimate to other methods, including a simple equal allocation of annual ET among the 12 months (and no accounting for monthly ΔM), and results did not differ substantially, so the method adopted here should not be thought to depend critically on the hydrological model climatology. Rather, it suggests that, at least for the Cascade region considered, variability in precipitation and runoff are dominant over variability in ET and soil moisture in determining the variability in snowpack. It also lends confidence to our approach, which relies on good measurements of the important quantities (precipitation and runoff), and assumptions about the less important ones (ET and soil moisture). Additionally, the finding by

31

Hamlet et al. (2007) that the timing of the ET and soil moisture annual cycles in the Pacific Northwest has not changed substantially since the early 20th century provides some assurance that our simple method is not missing an important ET/soil moisture-dependent contribution to climatic changes in the Cascades water balance.

With monthly values of all of the terms in (4), and assuming the snowpack starts out at zero in each water year, (4) is integrated in monthly increments to obtain a value of SWE volume at the end of each month. The monthly values are then converted to percent of the 1961-1990 mean 1 April value, yielding the final monthly time series of snowpack within the watershed subset for the period 1930-2007.

References

Allan, R., and T. Ansell, 2006: A new globally complete monthly historical gridded mean sea level pressure dataset (HadSLP2): 1850–2004. *J. Climate*, **19**, 5816–5842.

Barnett, T. P., D. W. Pierce, H. G. Hidalgo, C. Bonfils, B. D. Santer, T. Das, G. Bala, A W. Wood, T. Nozawa, A. A. Mirin, D. Cayan, M. D. Dettinger, 2008: Human-induced changes in the hydrology of the western United States. *Science*, **319**, 1080-1083.

Brohan, P., J. J. Kennedy, I. Harris, S. F. B. Tett and P. D. Jones, 2006: Uncertainty estimates in regional and global observed temperature changes: a new dataset from 1850. *J. Geophys. Res.*, **111** (D12106), doi:10.1029/2005JD006548.

Casola, J. H., L. Cuo, B. Livneh, D. P. Lettenmaier, M. T. Stoelinga, P. W. Mote, and J. M. Wallace, 2008: Assessing the impacts of global warming on snowpack in the Washington Cascades. Submitted to *J. Climate*.

Cayan, D.R., 1996: Interannual climate variability and snowpack in the western United States. *J. Climate*, **9**, 928–948.

Cayan, D. R., S. A. Kammerdiener, M. D. Dettinger, J. M. Caprio, and D. H. Peterson, 2001: Changes in the onset of spring in the western United States. *Bull. Amer. Meteor. Soc.*, **82**, 399–415.

Dodson, M., and co-authors, 2004: Oregon strategy for greenhouse gas reductions. Oregon Department of Energy, 192 pp.

Durre, I., R. S. Vose, and D. B. Wuertz, 2006: Overview of the Integrated Global Radiosonde Archive. *J. Climate*, **19**, 53-68.

Elsner, M. M., L. Cuo, N. Voisin, J. S. Deems, A. F. Hamlet, J. A Vano, K. E. B Mickelson, S.-Y. Lee, and D. P. Lettenmaier, 2009: Implications of 21st century climate change for the hydrology of Washington state. Chapter 3 in *The Washington Climate Change Impacts Assessment*, J. Littell, M. M. Elsner, L. W. Whitley, and A. Snover, Eds., Climate Impacts Group, University of Washington, pp 3.1-3.66.

Guilyardi, E., 2006: El Niño-mean state-seasonal cycle interactions in a multi-model ensemble. *Clim. Dynam*., **26**, 329–348.

Hamlet, A. F., P. W. Mote, M. P. Clark, and D. P. Lettenmaier, 2005: Effects of temperature and precipitation variability on snowpack trends in the western U.S. *J. Climate*, **18** , 4545-4561.

Hamlet, A. F., P. W. Mote, M. P. Clark, and D. P. Lettenmaier, 2007: Twentieth-century trends in runoff, evapotranspiration, and soil moisture in the western United States. *J. Climate*, **20**, 1468-1486.

Hansen, J.E., R. Ruedy, Mki. Sato, M. Imhoff, W. Lawrence, D. Easterling, T. Peterson, and T. Karl, 2001: A closer look at United States and global surface temperature change. *J. Geophys. Res.*, **106**, 23947-23963, doi:10.1029/2001JD000354.

Karl, T. R., C. N. Williams Jr., F. T. Quinlan, and T. A. Boden, 1990: United States Historical Climatology Network (HCN) serial temperature and precipitation data. Carbon Dioxide Information and Analysis Center, Environmental Science Division Publication No. 3404, Oak Ridge Laboratory, 389 pp.

Lettenmaier, D.P., 1976: Detection of trends in water quality data from records with dependent observations. *Water Resour. Res*., **12**, 1037-1046.

Liang, X., D. P. Lettenmaier, E. F. Wood, and S. J. Burges, 1994: A simple hydrologically based

    model of land surface water and energy fluxes for general circulation models. *J. Geophys.*

    Res., **99** (D7), 14,415-14,428.

Mantua, N. J., S. R. Hare, Y. Zhang, J. M. Wallace, and R. C. Francis, 1997: A Pacific

    interdecadal climate oscillation with impacts on salmon production. *Bull. Amer. Meteor.*

    Soc., **78**, 1069-1079.

Mote, P. W., 2003: Trends in snow water equivalent in the Pacific Northwest and their climatic

    causes. *Geophys. Res. Lett.*, **30**, 1601, doi:10.1029/2003GL017258.

Mote, P. W., 2006: Climate-driven variability and trends in mountain snowpack in western North

    America. *J. Climate*, **19**, 6209–6220.

Mote, P. W., A. F. Hamlet, M. P. Clark, and D. P. Lettenmaier, 2005: Declining mountain

    snowpack in western North America. *Bull. Amer. Meteor. Soc.*, **86**, 39–49.

Mote, P. W., A. Hamlet, and E. Salathé, 2008: Has spring snowpack declined in the Washington

    Cascades? *Hydrol. Earth Syst. Sci.*, **12**, 193-206.

Overland, J. E., and M. Wang, 2007: Future climate of the North Pacific Ocean. *Eos Trans. AGU*,

    88(16), 178.

Panofsky, H. A., and G. W. Brier, 1963: *Some Applications of Statistics to Meteorology*. 1st ed.,

    The Pennsylvania State University, 224 pp.

Pierce, D. W., T. P. Barnett, H. G. Hidalgo, T. Das, C. Bonfils, B. D. Santer, G. Bala, M. D.

    Dettinger, D. R. Cayan, A. Mirin, A. W. Wood, T. Nozawa, 2008: Attribution of declining

    western U.S. snowpack to human effects. *J. Climate*, **21**, 6425–6444.

Regonda, S. K., B. Rajagopalan, M. Clark, and J. Pitlick, 2005: Seasonal cycle shifts in

    hydroclimatology over the western United States. *J. Climate*, **18**, 372–384.

Slack, J. R., and Landwehr, J. M., 1992: Hydro-climatic data network (HCDN): A U.S. Geological

Survey streamflow data set for the United States for the study of climate variations, 1874-

1988. *U.S. Geological Survey Open-File Report 92-129*, 193 pp.

Stewart, I.T., D.R. Cayan and M.D. Dettinger, 2005: Changes toward earlier streamflow timing

across western North America. *J. Climate,* **18**,1136-1155.

Trenberth, K. E., and J. W. Hurrel, 1994: Decadal atmosphere-ocean variations in the Pacific.

Climate Dyn., **9**, 303-319.

Wallace, J.M., and D.S. Gutzler, 1981: Teleconnections in the geopotential height field during the

Northern Hemisphere winter. *Mon. Wea. Rev.*, **109**, 784–812.

Wood, A.W. and D. P. Lettenmaier, 2006: A testbed for new seasonal hydrologic forecasting

approaches in the western U.S. *Bull. Amer. Meteor. Soc.*, **87**, 1699-1712.

van den Dool, H. M., S. Saha, and Å. Johansson, 2000: Empirical orthogonal teleconnections. *J.

Climate*, **13**, 1421-1435.

Table 1. Trends in 1 April snowpack associated with terms in the multiple linear regression of 1 April snowpack with winter precipitation (P) and winter 850-hPa temperature during onshore flow (T_{850ons}).

	Snowpack Change (%)		
	1930-2007	1950-1997	1976-2007
Actual Trend	-23	-48	+19
P part only (T_{850ons} held constant)	+2	-14	+13
T_{850ons} part only (P held constant)	-13	-22	+1
Full regression equation	-12	-36	+14
Residual	-11	-13	+5
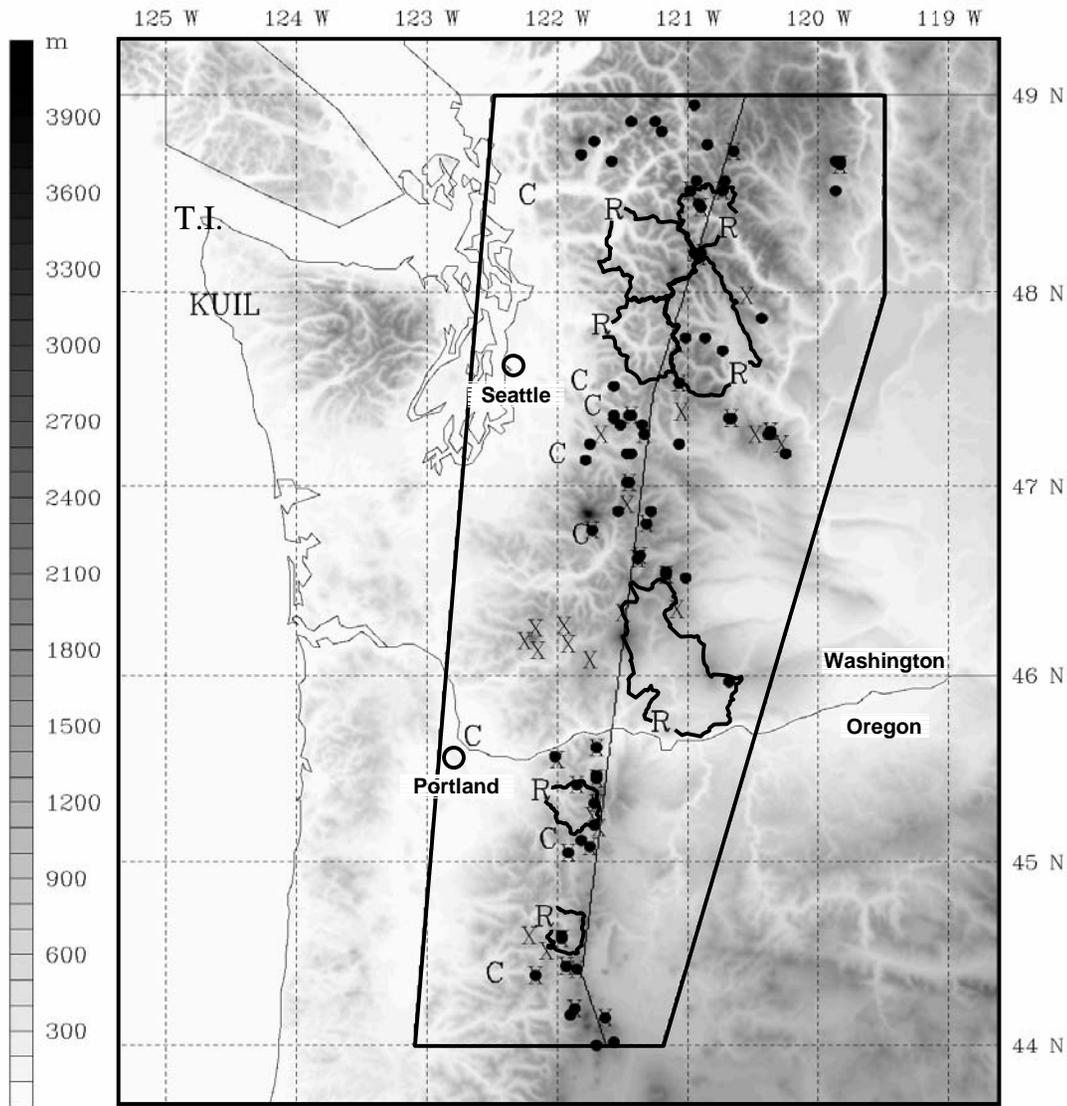
Figure 1. Map of study area. Heavy solid polygon defines "Cascade Mountains" for the purposes of this study. The thin solid line divides the Cascade Mountains into west-of-crest and east-of-crest regions. Filled black dots are locations of qualifying snow course sites for the observational snowpack verification data set, "X"s mark qualifying SNOTEL sites, "C"s marks qualifying USHCN temperature/precipitation sites, and "R"s marks qualifying HCDN streamflow gauge sites, with adjacent solid curves outlining the associated watersheds (or "watershed subset" referred to in text). "KUIL" and "T.I." mark the Quillayute and Tatoosh Island NWS upper air sites used to define T_{850ons}.
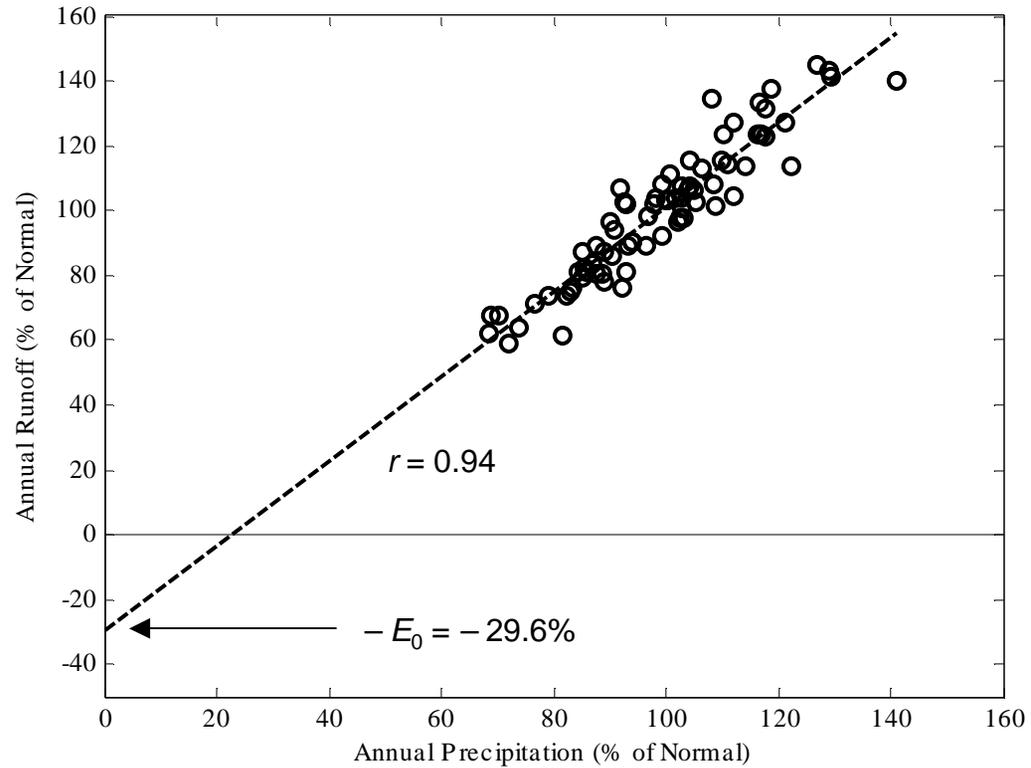
Figure 2. Scatter plot of annual runoff within the watershed subset (in percent of 1961-1990 mean) vs. west Cascade-averaged annual precipitation (also in percent of 1961-1990 mean). Also shown is best-fit line, correlation, and *y*-intercept.
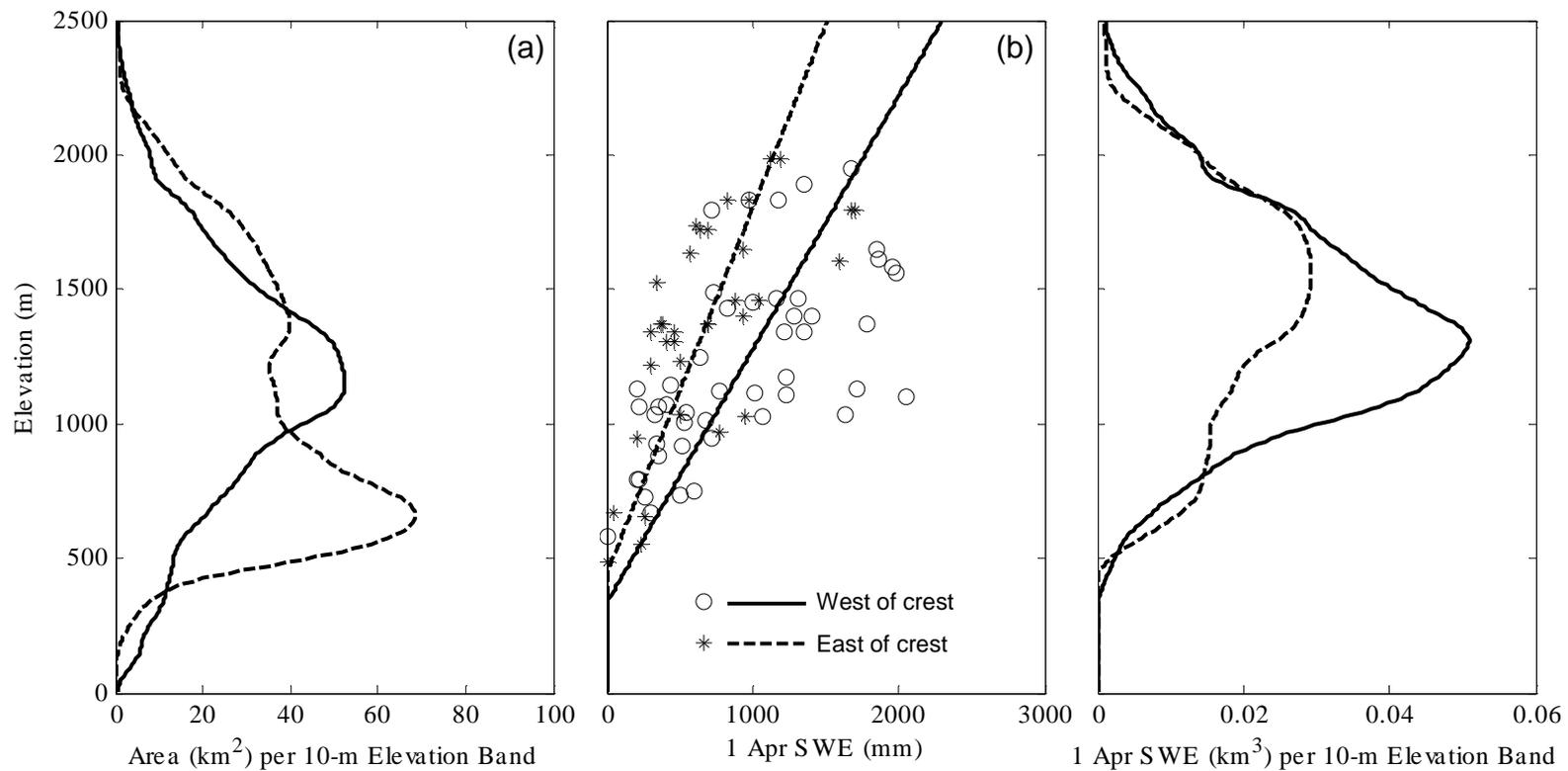
Figure 3. Example (for 1 April 2006) of information used to construct the snow course-based Cascade SWE volume used to verify the water-balance snowpack. (a) Total area covered by each 10-m elevation band (equivalent to the derivative with respect to height of the hypsometric curve) within the watershed subset shown in Fig. 1. Separate curves are shown for portions of the watersheds that are west and east of the crest, as defined by the polygons in Fig. 1. (b) Scatter plot of SWE depth vs. elevation, with linear fits, for stations west and east of the crest. (c) Estimate of SWE volume vs. elevation within the watershed subset, obtained by multiplying (a) x (b).
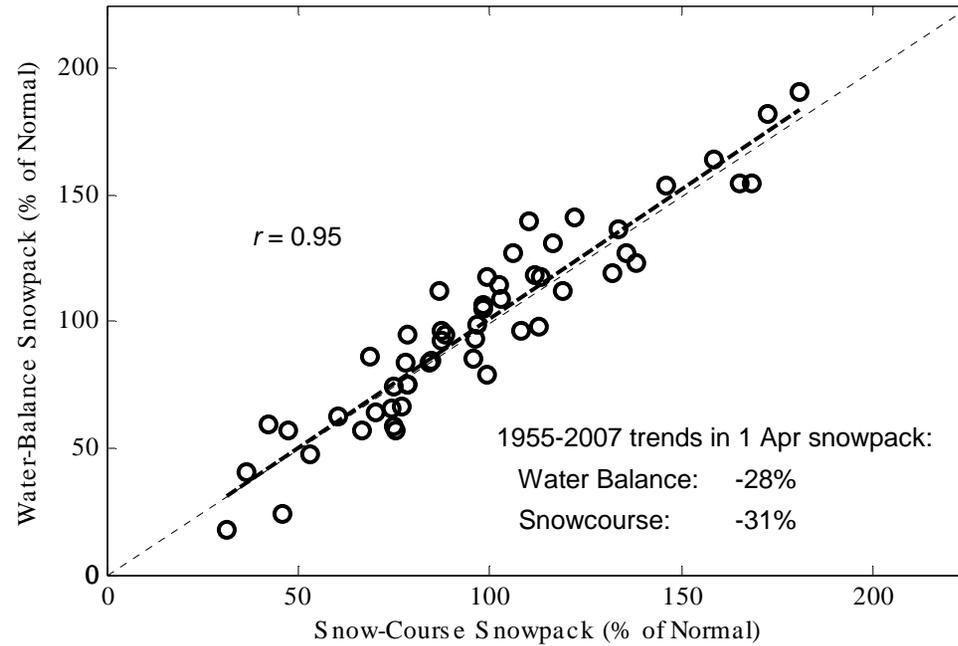
Figure 4. Scatter plot of water-balance 1 April snowpack vs. snow-course 1 April snowpack, for years 1955-2007 (1955 was the first year of the snow-course snowpack time series). Values are in percent of 1961-1990 normal for SWE volume in the Cascade watershed subset. Also shown is the 1:1 line (thin dashed), the best-fit line (heavy dashed) with correlation, and the 1955-2007 trend values.
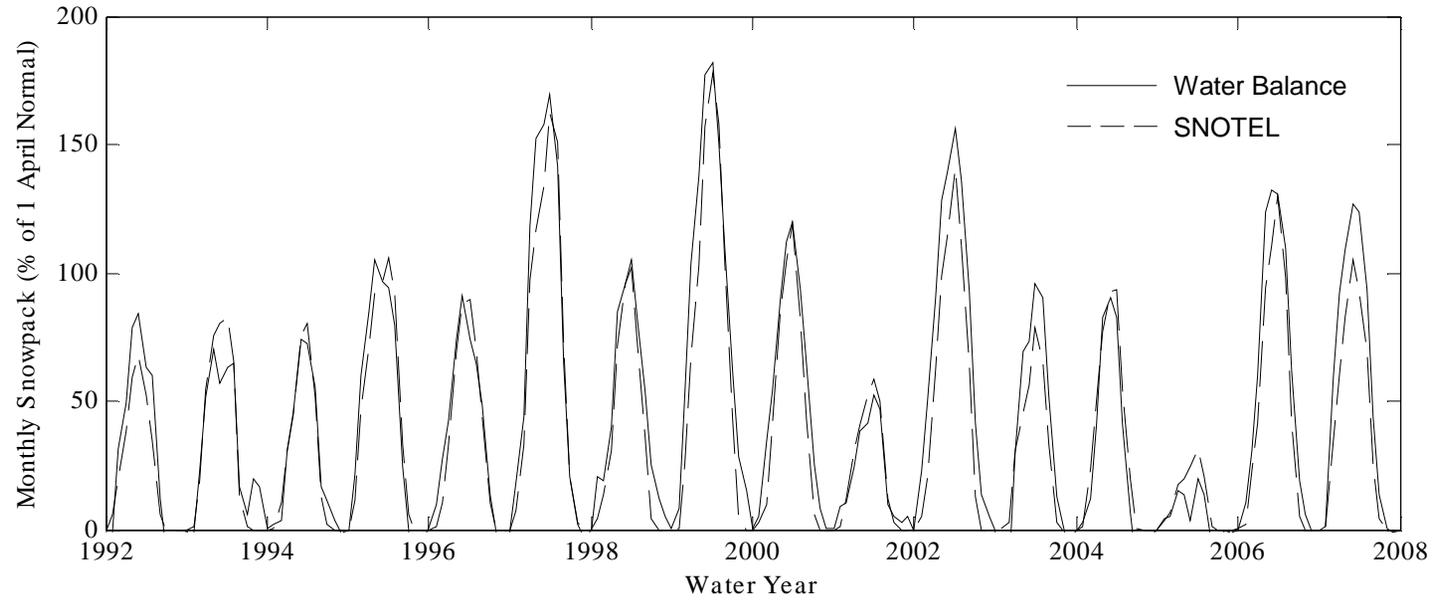
Figure 5. Monthly snowpack derived from the water-balance model (solid) and from SNOTEL observations (dashed), expressed as a percent of the 1961-1990 normal 1 April SWE volume for the watershed subset, for water years 1992 through 2007. Water years are labeled at October 1 (the start of the water year).
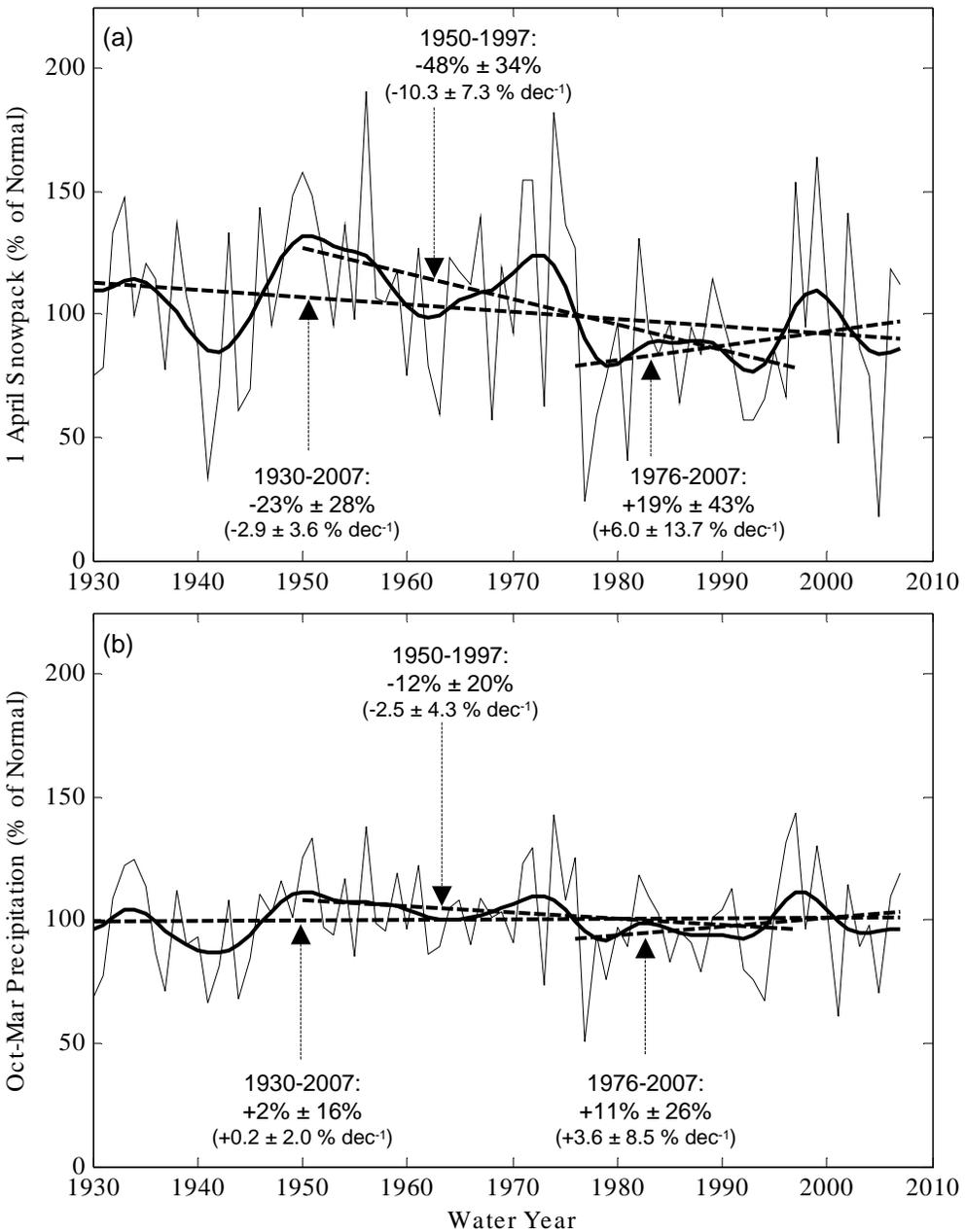
Figure 6. (a) 1 April water-balance snowpack (% of 1961-1990 mean, thin solid curve); smoothed version (heavy solid curve); trend lines over the periods indicated (heavy dashed lines), with trend values (given in total percent change and percent per decade) and 95% confidence intervals listed. (b) As in (a), except for October-March west Cascade-averaged precipitation (% of 1961-1990 mean). (c) As in (a), except for November-March west Cascade-averaged temperature anomaly (°C). (d) As in (a), except for November-March mean 850-hPa temperature anomaly (°C) at KUIL when 850-hPa flow is onshore. Temperature anomalies are with respect to the 1961-1990 mean.
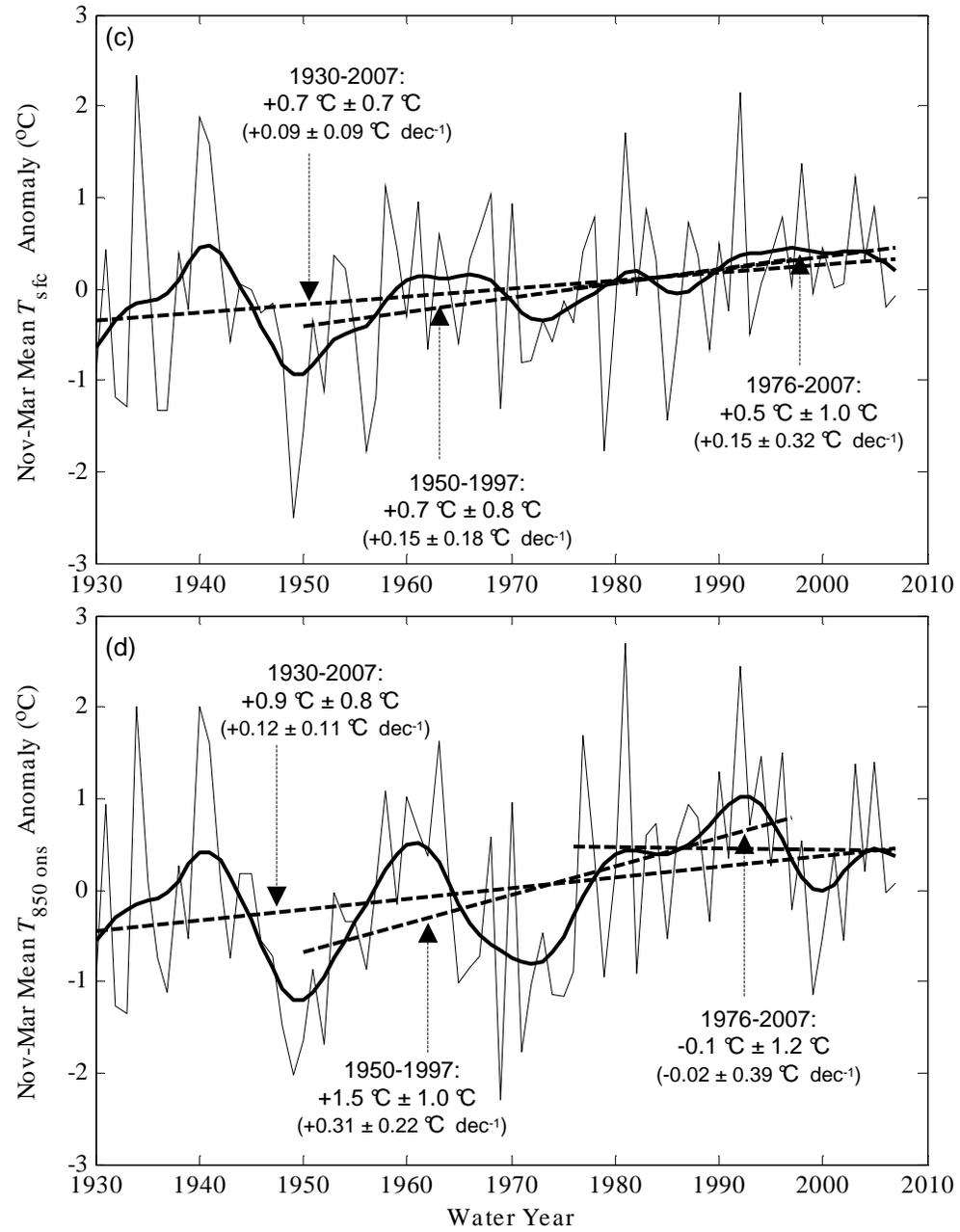
Figure 6 (cont.).
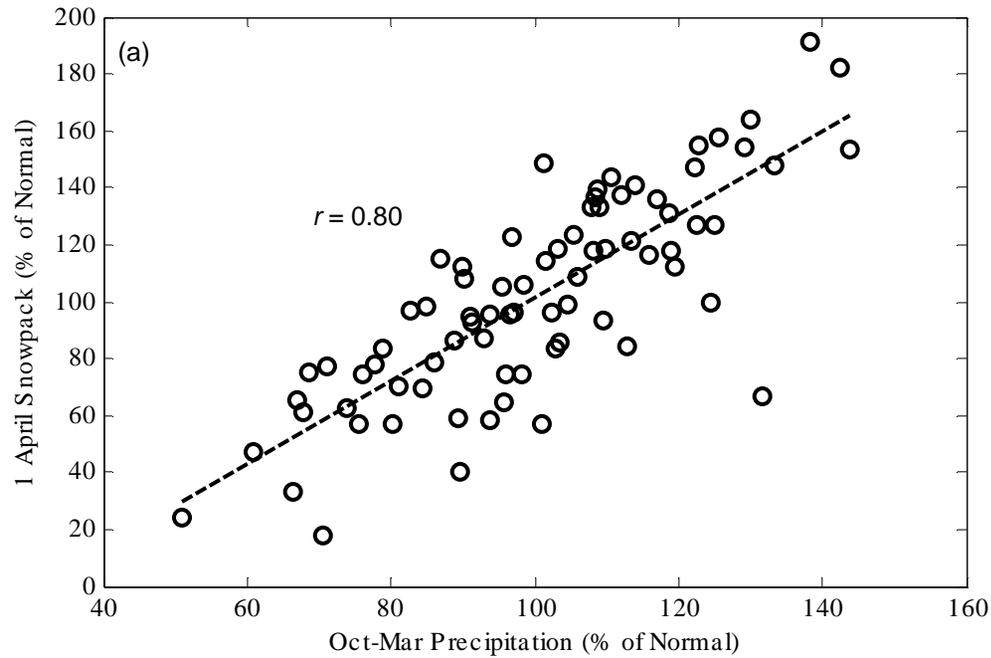
Figure 7. (a) Scatter plot of water-balance 1 April snowpack vs. October-March west Cascade-averaged precipitation (both as % of 1961-1990 mean). (b) Scatter plot of water-balance 1 April snowpack vs. November-March west Cascade-averaged temperature anomaly (°C). (c) Scatter plot of water-balance 1 April snowpack vs. November-March mean 850-hPa temperature anomaly (°C) at KUIL when 850-hPa flow is onshore.
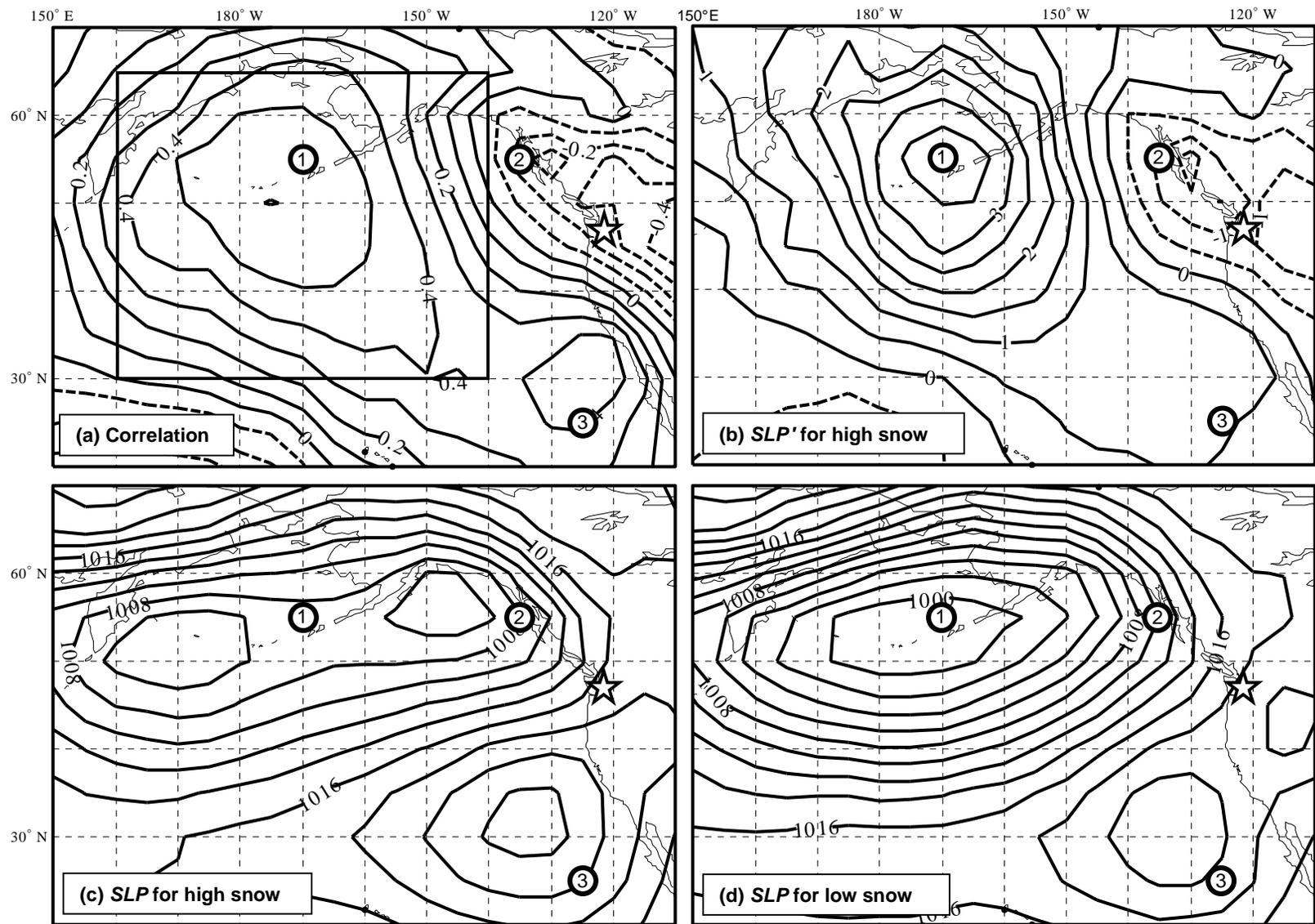
(b)

$r = -0.44$

1 April Snowpack (% of Normal)

Nov-Mar Mean T_{sfc} Anomaly (^{o}C)

(c)

$r = -0.68$

1 April Snowpack (% of Normal)

Nov-Mar Mean $T_{850 ons}$ Anomaly (^{o}C)
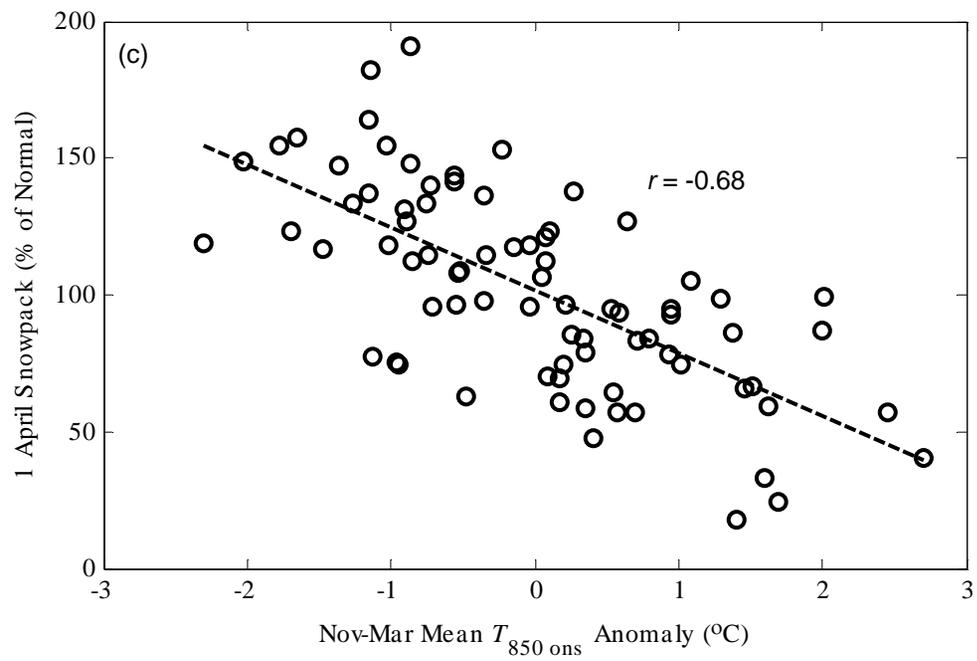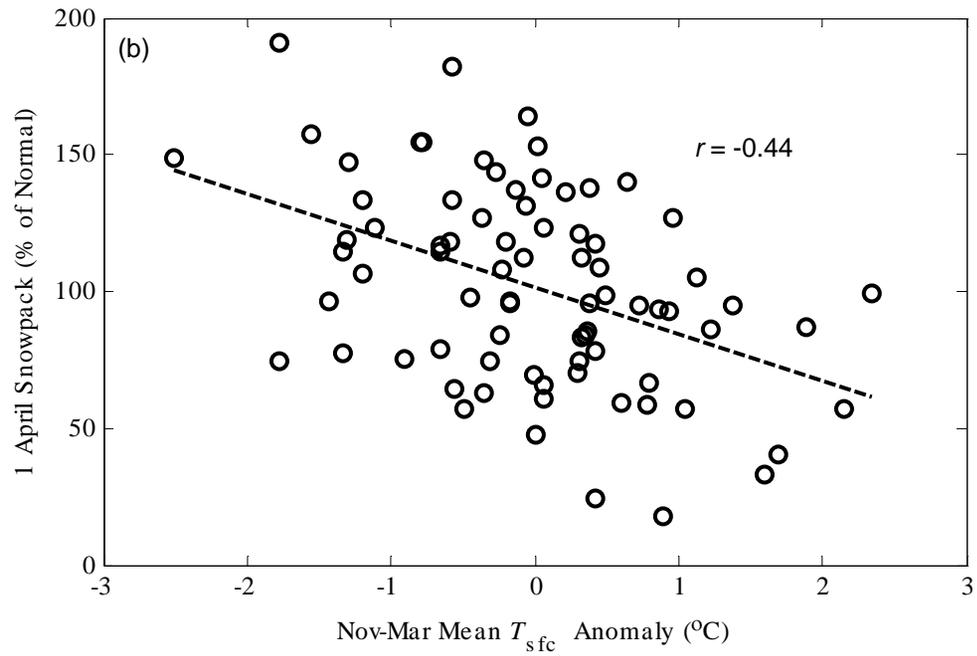
Figure 7 (cont.).

Figure 8. (a) Map of the regression coefficient between the winter (November-March mean) sea-level pressure field over the north Pacific Ocean region and the Cascade 1 April snowpack (from the water-balance). Location of Cascade Range indicated by star. Numbered circles indicate the set of three points within the domain whose SLP explains more of the variance in snowpack than any other set of three points. Box shows averaging area for the North Pacific Index (NPI). (b) Composite of the winter SLP anomaly field (hPa, as a departure from the 1961-1990 mean) during the five years with highest Cascade Snow Circulation (CSC) index. (c) Composite of the total winter SLP field (hPa) during the five years of highest CSC index. (d) Composite of the total winter SLP field (hPa) during the five years of lowest CSC index.
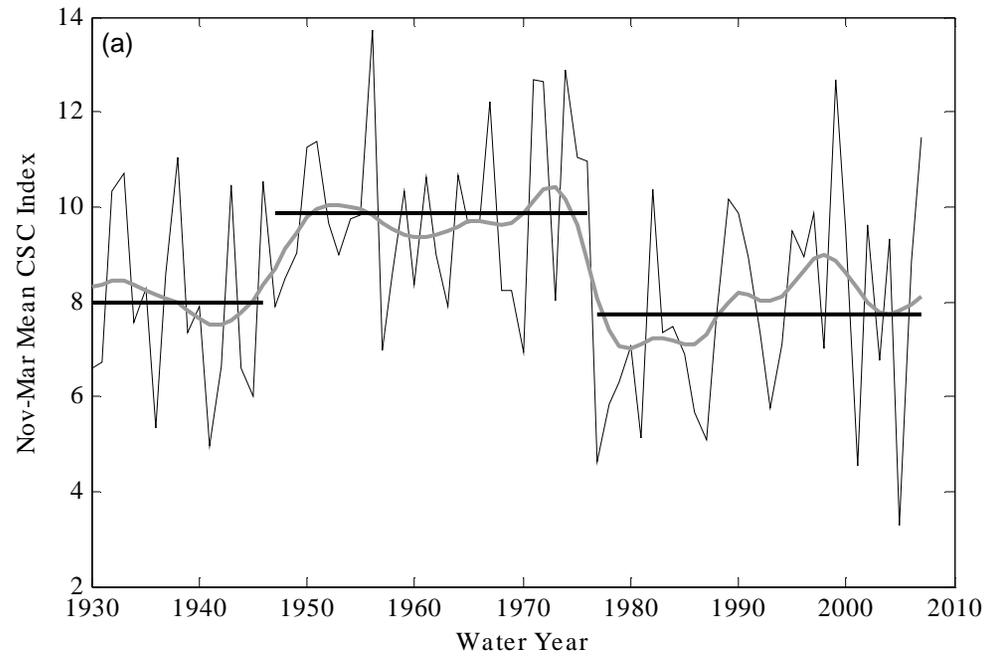
Figure 9. (a) Time series of November-March mean CSC index (hPa, thin black curve), smoothed version (heavy gray curve), and means of CSC index during PDO epoch periods (heavy black lines). (b) Scatter plot of 1 April snowpack (from the water-balance, in % of 1961-1990 mean) vs. November-March mean CSC index (hPa, black circles) with best-fit line (black dashed) and correlation. (c) As in Fig. 6a, except the snowpack time-series has had the CSC-correlated part removed.
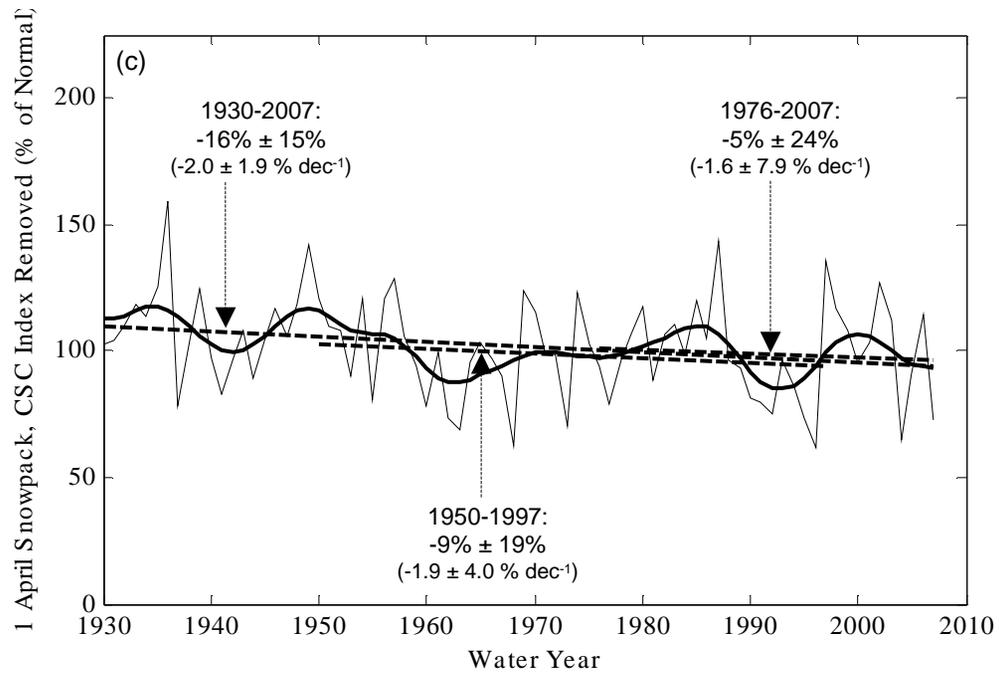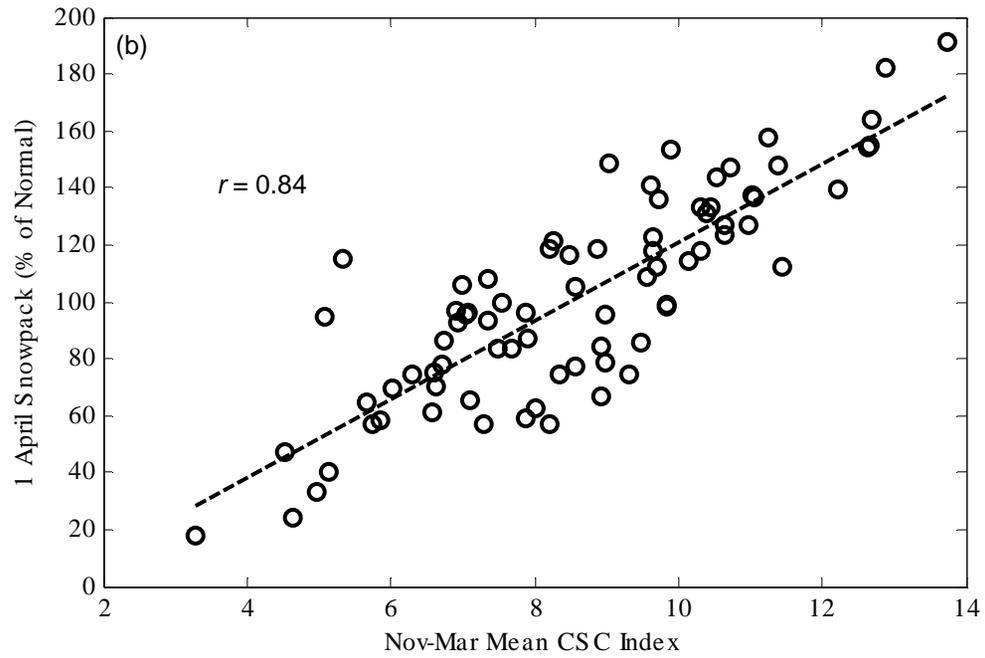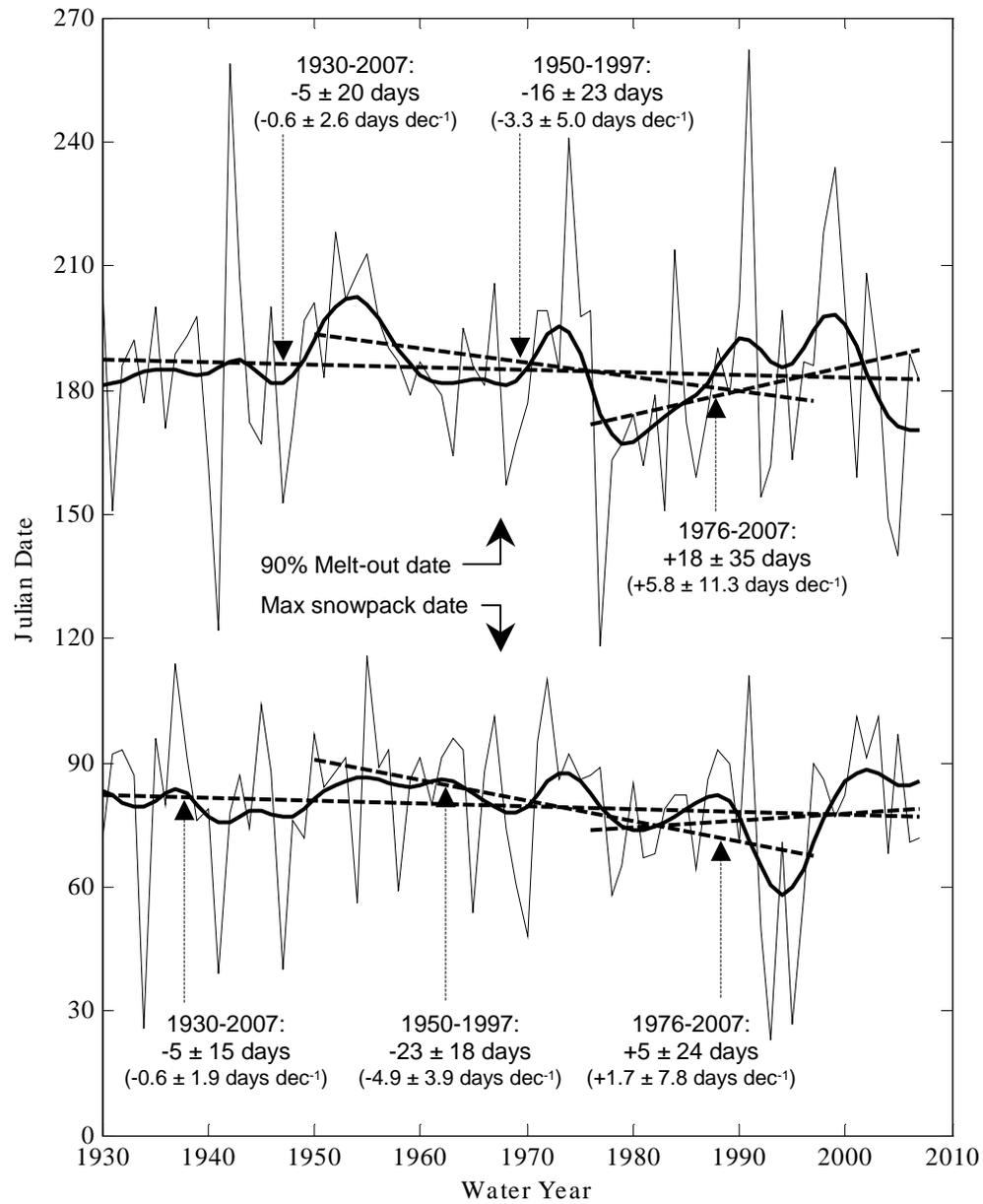
Figure 9 (cont.).

Figure 10. As in Fig. 6a, except showing Julian date of maximum snowpack (lower curves and lines) and of 90% melt-out (upper curves and lines), based on the water-balance monthly snowpack record.
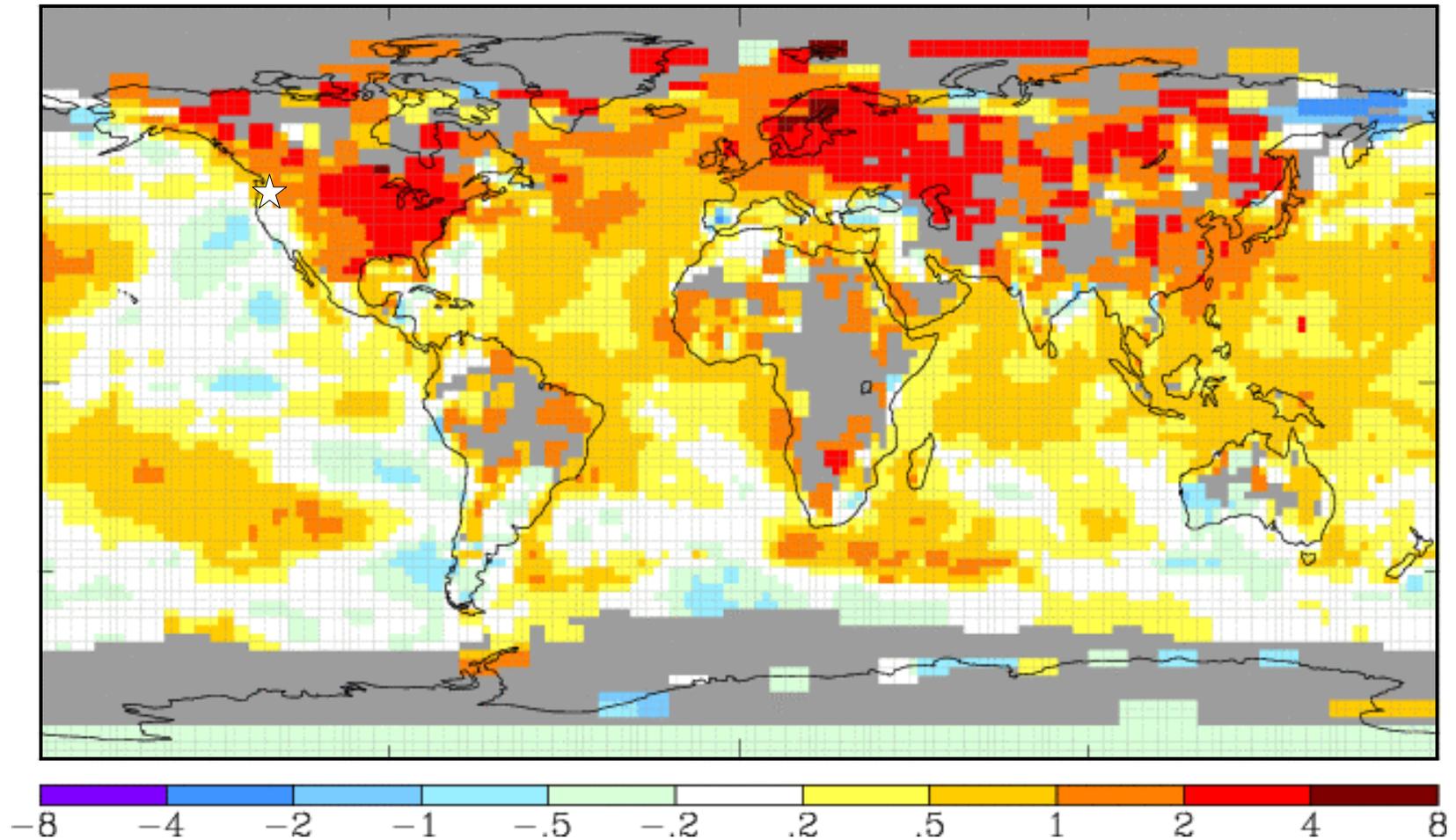
Figure 11. Changes in December-February mean surface air temperature (°C) during the period 1976 to 2007, based on linear trends. The plot was generated using the temperature trend mapping web page provided by the NASA Goddard Institute for Space Studies (http://data.giss.nasa.gov/gistemp/maps), which uses the surface temperature data set described by Hansen et al. (2001). The white 5-point star indicates the region of interest in the present study.
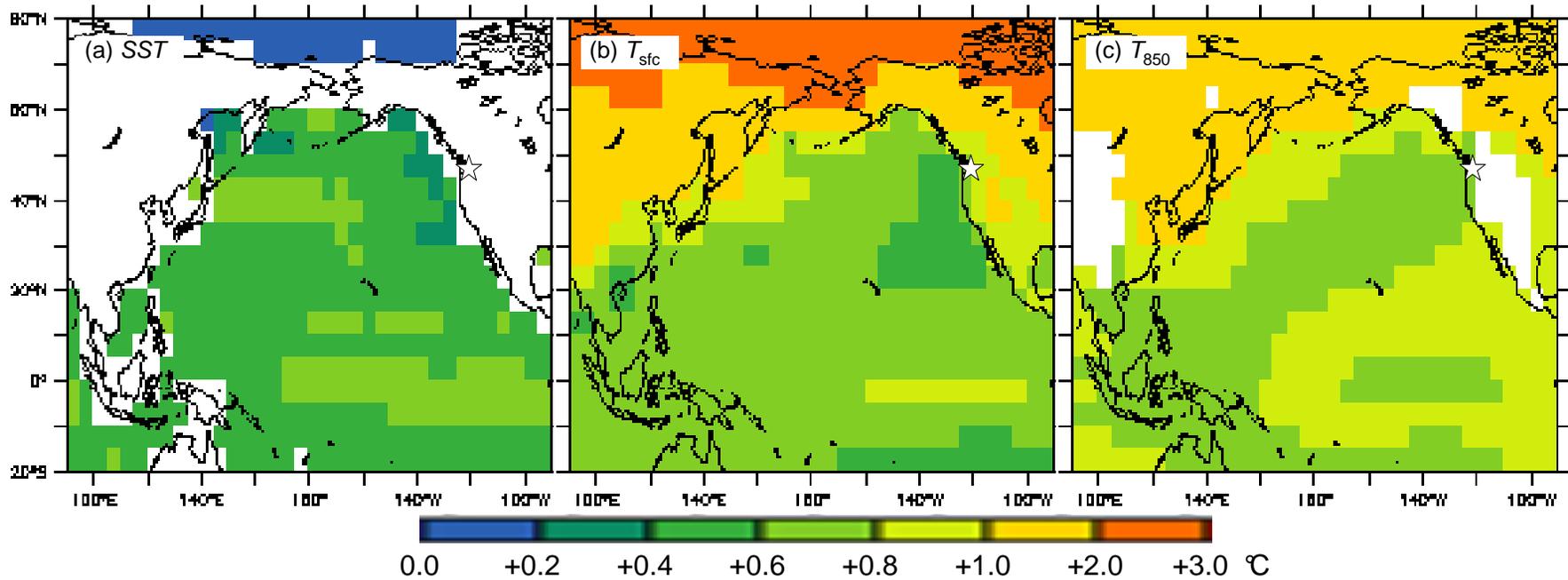
Figure 12. Predicted linear trend of November-March mean temperature for 1990 to 2025 (°C), as predicted by the Overland and Wang (2007) ensemble of climate model forecasts. Shown are the ensemble means of (a) sea-surface temperature, (b) surface air temperature, and (c) 850-hPa temperature. The white 5-point stars indicate the region of interest in the present study.
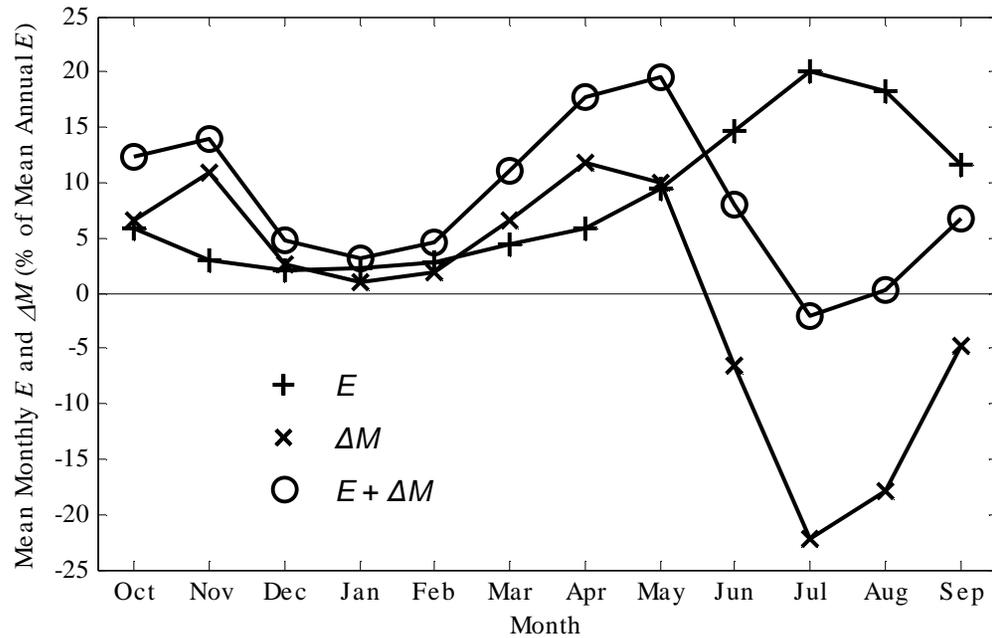
Figure 13. Climatological monthly values of evapotranspiration (*E*), change in soil moisture (*ΔM*), and the sum of the two, expressed as a percentage of the mean annual evapotranspiration, derived from VIC hydrological model simulations for four Cascade Mountain watersheds for the period 1971-2000.